

Boundary Layer Scheme Development for the UFS

Joseph Olson¹, Wayne Angevine^{2,3}, Jaymes Kenyon^{1,2}, Dave Turner¹,
John Brown¹, Siwei He^{1,2}, and Franciano Puhales⁴

¹ NOAA/Global Systems Laboratory

² Cooperative Institute for Research in Environmental Sciences

³ NOAA/Chemical Systems Laboratory

⁴ Universidade Federal de Santa Maria, Santa Maria, Brazil

Outline

- Questions Regarding an Optimal PBL Scheme Design
 - Brief Overview of MYNN-EDMF
- Recent Development Activities
 - Removal of numerical pathologies
 - Improving Clouds:
 - Addition of a high-order moment cloud PDF
 - Accelerating plume modification
- Future Work
- Summary

Main points

Performance of the MYNN-EDMF is good, but the development process matters as much or more

Our development process emphasizes performance in specific regimes identified as critical:

- Deep convection (severe weather)
- Shallow cumulus (renewable energy and air quality)
- Stable boundary layer (low temperatures, moisture transport by low-level jets)
- Marine stratocumulus (medium-range forecasting up to climate)
- Testing at all scales (global, regional, SCM)

We demonstrate deriving SCM forcing from operational RAP analyses, making additional cases easy to test once identified

We can run LES to compare variables not easily derived from limited observations

Questions for Optimal Scheme Design

- What is the most suitable design/framework to address the full set boundary-layer-related forecast challenges?
 - Which framework is the optimal “engine under the hood”: TKE- L , TTE, or TKE- ε , other?
 - Scientific optimality may be unknowable; Engineering maturity and flexibility are important
- What is the best approach to represent non-local mixing?
 - Mass-flux scheme or a higher-order closure (HOC; prognose more moments)?
 - Are these options incompatible with each other?
- Should shallow cumulus be embedded within the boundary-layer scheme or separate?
 - Eliminate all possible duplicate processes, arbitrary partitioning of processes, and streamlining for efficiency.
 - Separate schemes can be designed to limit duplicate processes and still be highly integrated.

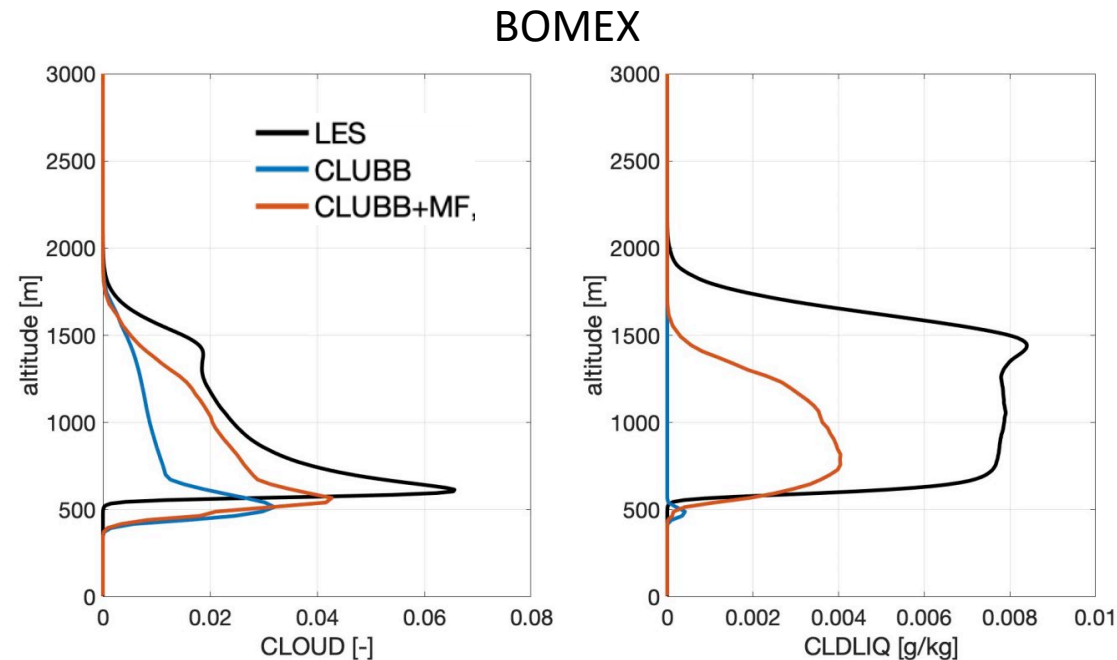
Status:
open question

Status:
open, but progress
has been made

Status:
probably can go
either way if both
bullets are
satisfied

Using both H.O.C and Mass Flux

- While most operational forecast centers have employed EDMF schemes, the higher-order closure scheme **Cloud Layers Unified By Binomials (CLUBB)** scheme has shown benchmark-level success in the representation of *stratocumulus*
 - Attributable to the use of high-order moments in cloud PDFs
- The primary limitation of CLUBB is computational expense
 - Not a limitation for mass-flux schemes (EDMF approach)
- Recent results from Mikael Witte et al. (JPL) show that *shallow cumulus* clouds in CLUBB can be improved with the addition of a mass-flux scheme
 - Better shallow cumulus depth, mixing ratio, and variability
- A data point to suggest the combination of the use of high-order moments with a mass-flux scheme may be the most computationally efficient approach to get both stratocumulus and shallow cumulus clouds well represented



Adapted from Witte et al. (2021) - Improvement and Calibration of Clouds in Models, Toulouse, France

A very brief overview of the
MYNN-EDMF

Mellor-Yamada-Nakanishi-Niino Eddy Diffusivity-Mass Flux (MYNN-EDMF) Turbulence Scheme

- **Has been used in NOAA's operational RAP and HRRR forecast systems since 2014**

- **The main features include:**

- **Eddy Diffusivity-Mass Flux (EDMF) scheme:**

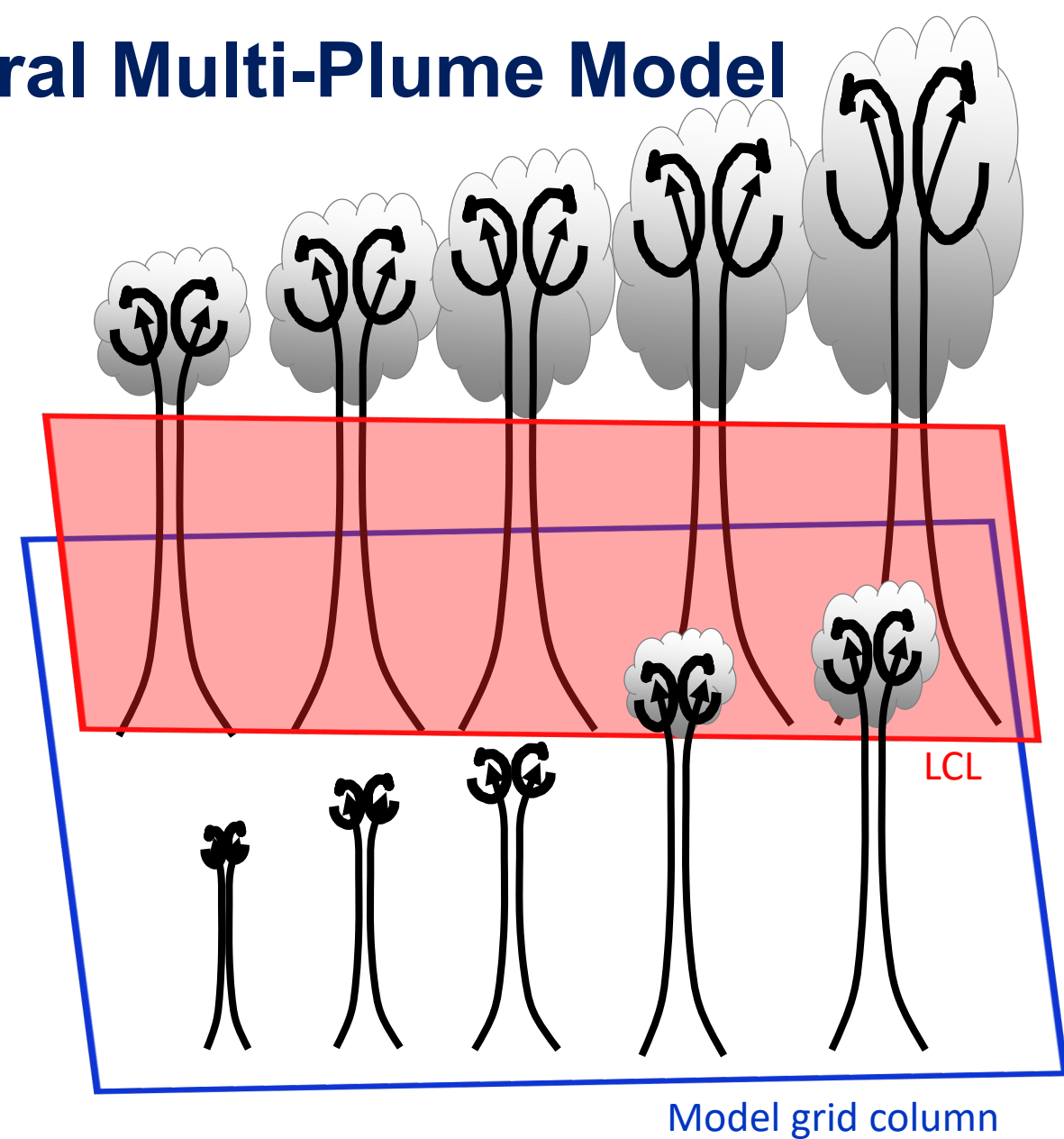
$$\overline{w'\phi} = -K \frac{\partial \bar{\phi}}{\partial z} + M(\phi_u - \bar{\phi})$$

- **Eddy Diffusivity:** turbulent kinetic energy (TKE)-based with option to run at level 2.5, 2.6, or 3.0 closure
- **Mass Flux:** dynamic spectral multi-plume model (Neggers 2015, *JAMES*)
- **Moist-turbulent mixing scheme:**
 - Moist conserved variables θ_{li} [$= \theta - (\theta/T)(L_v/c_p)q_l - (\theta/T)(L_f/c_p)q_i$] and q_w ($= q_v + q_l + q_i$), are used as thermodynamic variables
 - Uses cloud PDFs to represent both stratus and convective **subgrid-scale (SGS) clouds**, their **impact on turbulent mixing**, and the SGS clouds are **coupled to the radiation scheme**
- **Other distinguishing aspects:**
 - Originally and continually tuned to a wide variety of LES simulations
 - The critical Richardson number for momentum has been removed, similar to TTE schemes
 - Mass-flux scheme is designed to parameterize all non-local mixing (dry and cloudy) in all environments and represent the impacts of shallow cumulus (cloud production, turbulent transport, and subsidence)

MYNN-EDMF: Dynamic Spectral Multi-Plume Model

A **spectral plume model** is used to explicitly represent all plume sizes that are likely to exist in a given atmospheric state, following **Neggers (2015, JAMES)** and **Suselj et al. (2013, JAS)**.

- Total maximum number of plumes possible in a single column: **10**
- Diameters (ℓ): **100, 200, 300, 400, 500, 600, 700, 800, 900, and 1000 m**
- Max plume size is **MIN(PBLH, cloud ceiling, Δx)**
- Plumes are only active when:
 - Superadiabatic in lowest 50 m
 - Positive surface heat flux
- Plumes condense only if they surpass the **lifting condensation level (LCL)**



MYNN-EDMF: Individual Plume Integration

The vertical integration of each plume is performed with an entraining bulk plume model for the variables $\phi = \{\theta_{ij}, q_t, u, v, \text{ and TKE}\}$ using a simple entraining rising parcel:

$$\frac{\partial \phi_{ui}}{\partial z} = -\varepsilon_i (\phi_{ui} - \phi)$$

where ε_i is the fractional entrainment rate, which regulates the lateral mixing of the updraft properties, ϕ_{ui} , with the surrounding air, ϕ . The vertical velocity equation uses a form from Simpson and Wiggert (1969), with the buoyancy $B = g(\theta_{v,ui} - \theta_v)/\theta_v$ as a source term:

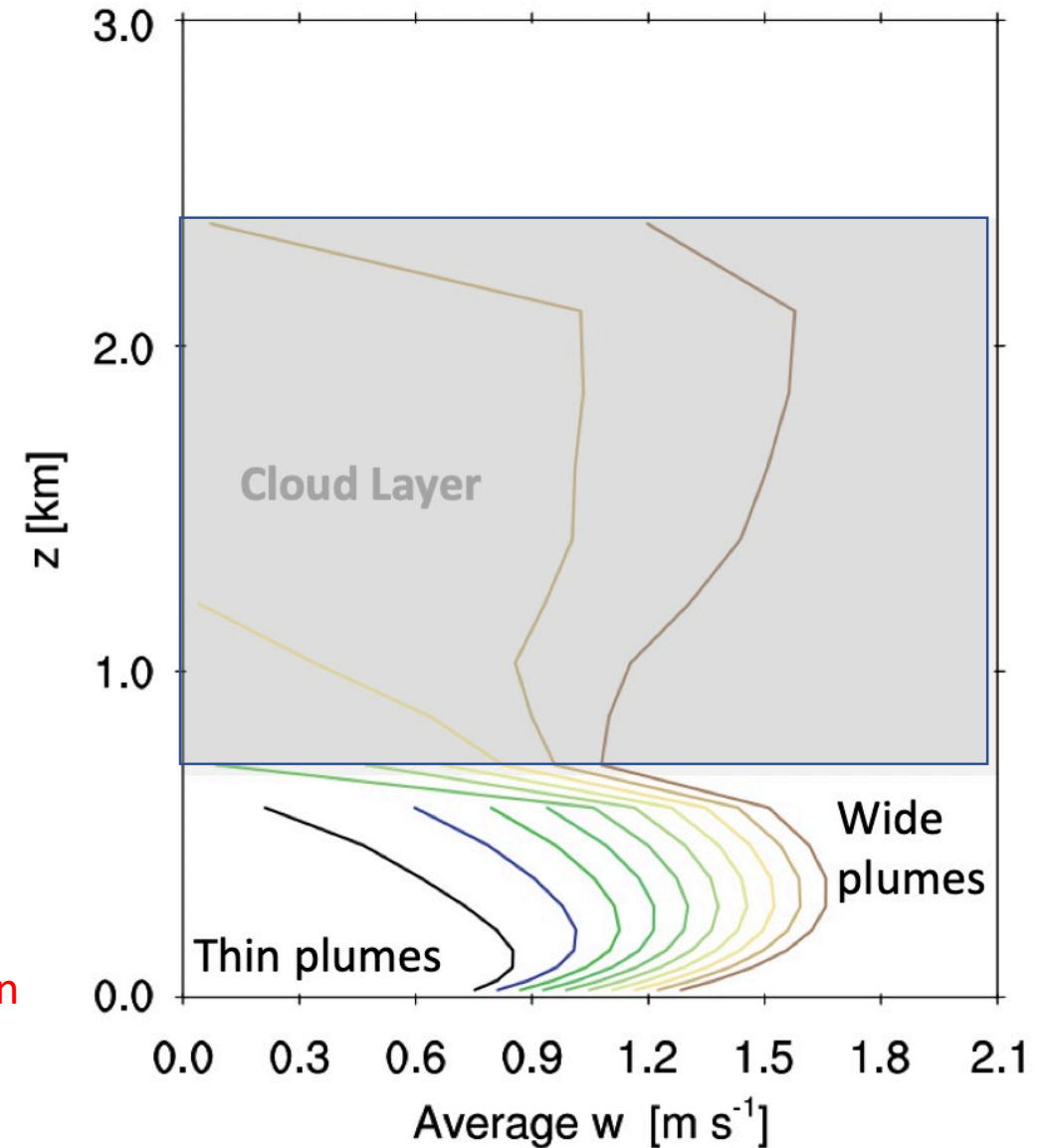
$$w_{ui} \frac{\partial w_{ui}}{\partial z} = -\varepsilon_i a w_{ui}^2 - bB$$

The only distinguishing aspect to each plume is the entrainment rate ε_i , which is taken from Tian and Kuang (2016):

$$\varepsilon_i = \frac{C_\varepsilon}{w_i l_i}$$

Where l_i is the plume diameter, and $C_\varepsilon = 0.33$.

Note: This form can produce a positive feedback



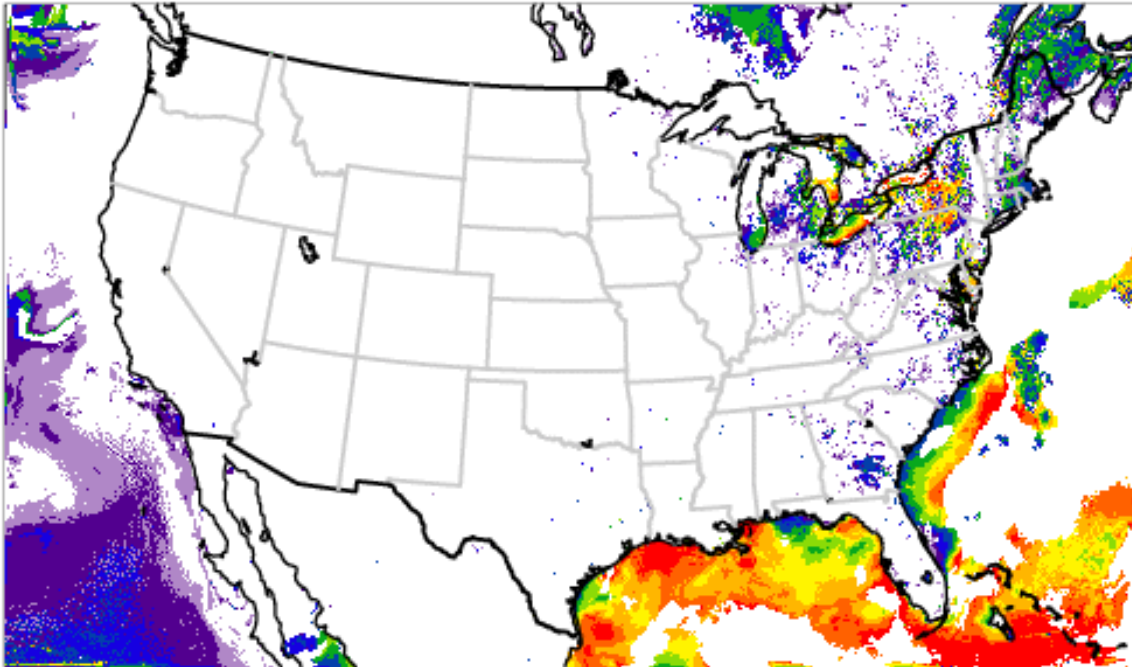
Adapted from Neggers (2015, JAMES)

Example of Dynamic Spectral Mass-Flux Scheme

HRRR 18-hour forecast
Valid times: 12 UTC 24 June – 03 UTC 25 June 2020

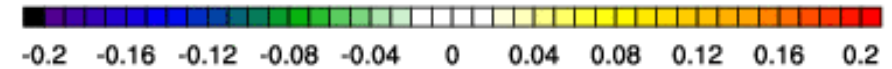
HRRR
Number of active plumes

Init: 2020-06-24_09:00:00
Valid: 2020-06-24_12:00:00



HRRR
Maximum mass flux in column (m s^{-1})

Init: 2020-06-24_09:00:00
Valid: 2020-06-24_12:00:00



Negative = dry

Positive = condensing

Example Comparison of SW-up at Top of Atmosphere

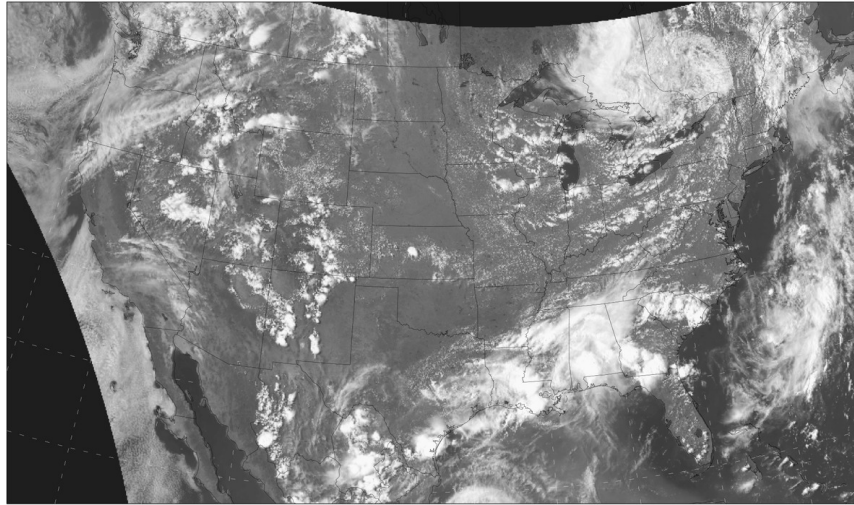
21 UTC 24 June 2020

Forecast hour 12, Initialized 09 UTC 24 June 2020

**GOES-16
Satellite**

GOES-16 combined (ch1, 2, 3) visible albedo

20:52:35 24 Jun 2020

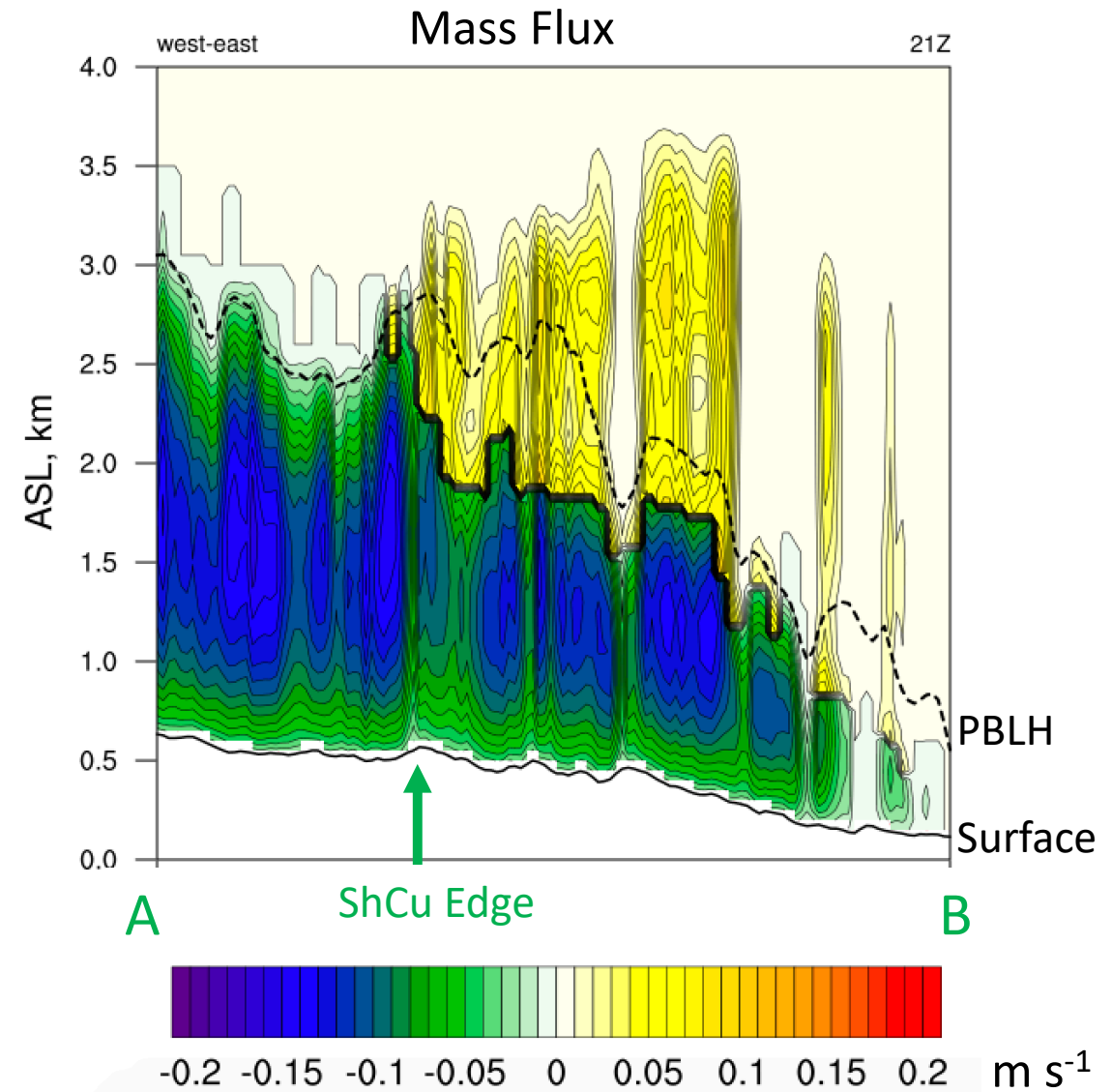
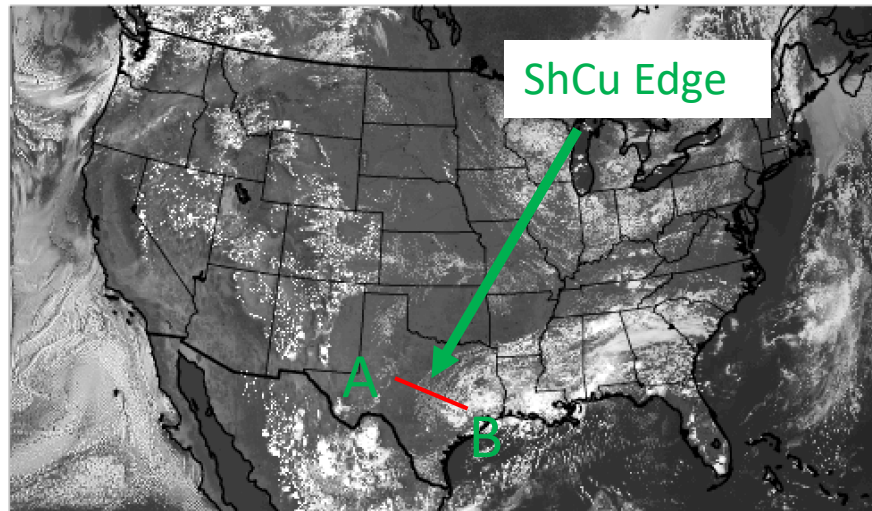


HRRR

Upward SW at TOA ($W m^{-2}$)

Init: 2020-06-24_09:00:00

Valid: 2020-06-24_21:00:00



Dry portion of plumes

Moist portion of plumes

**Both Stratus +
Mass-Flux
Components
active**

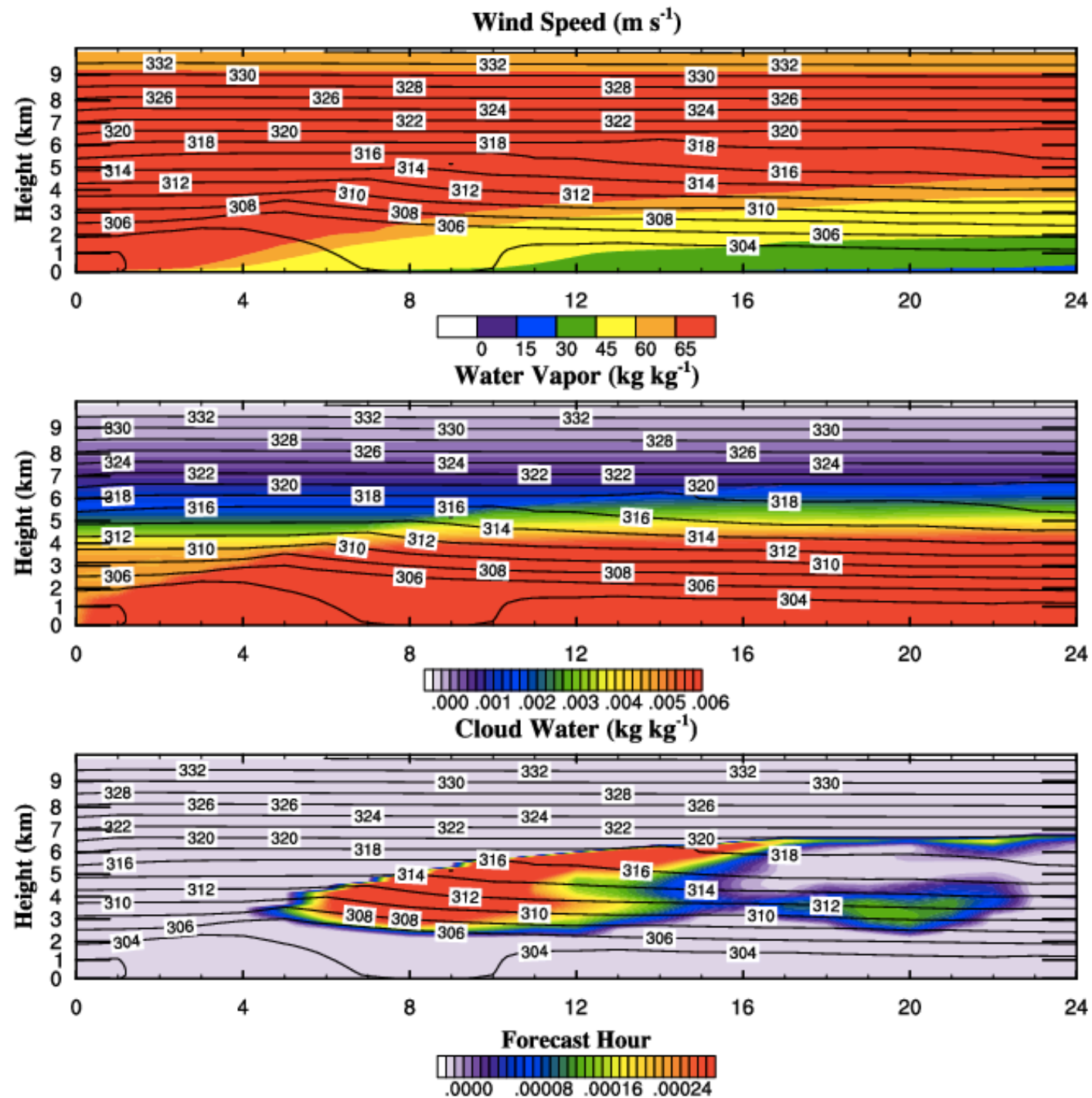
Recent Development Activities:
Removing Numerical
Pathologies in the MYNN-EDMF

Stress Test: Hurricane SCM case

- No diurnal cycle
- Over land
- 60 m s^{-1} wind speeds
- Moderate/Low background moisture
- Clouds develop after hour 4

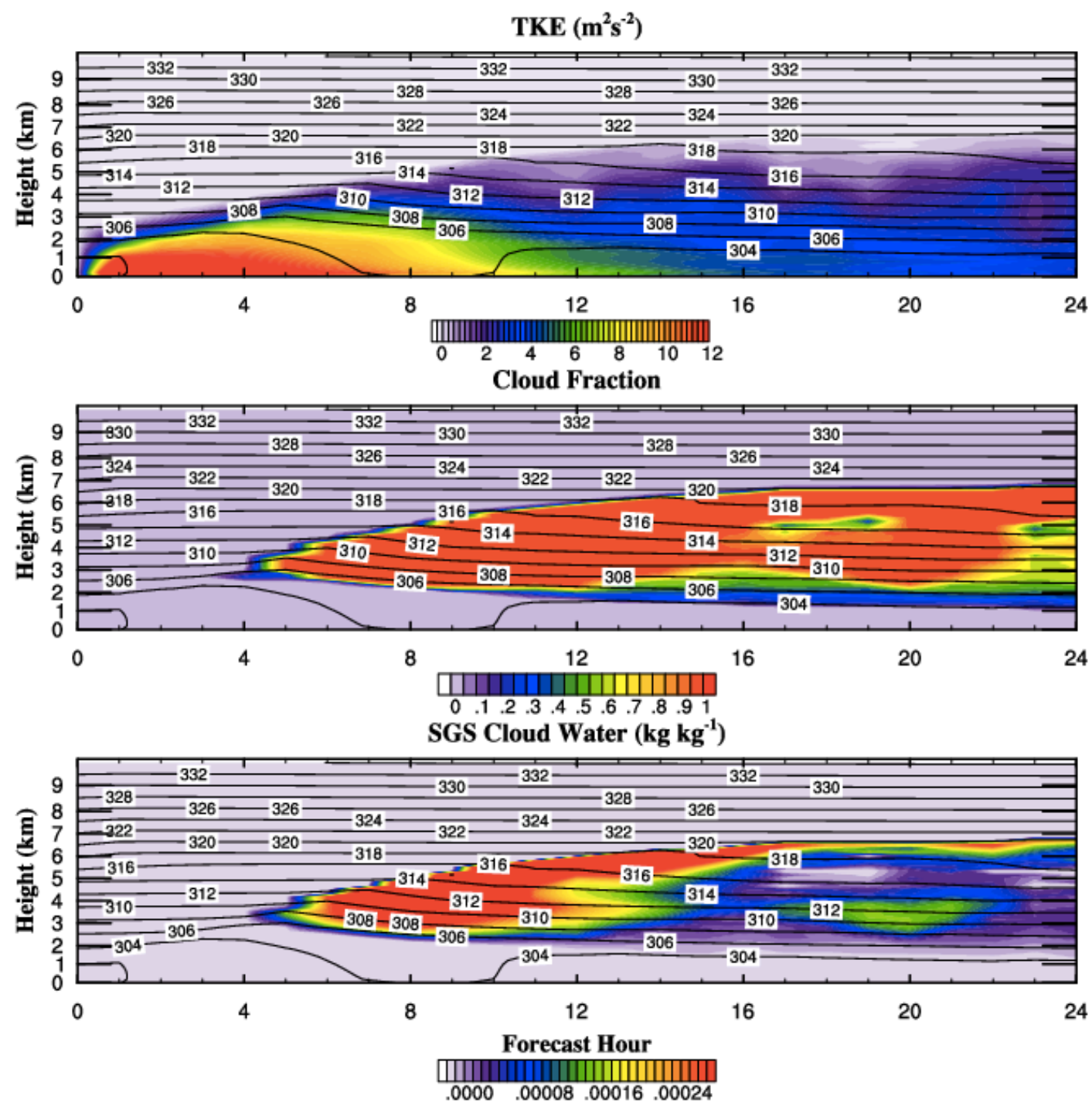
Configuration:

- $\Delta x=2 \text{ km}$, $\Delta t=15 \text{ sec}$
- MYNN-EDMF
- MYNN surface layer scheme

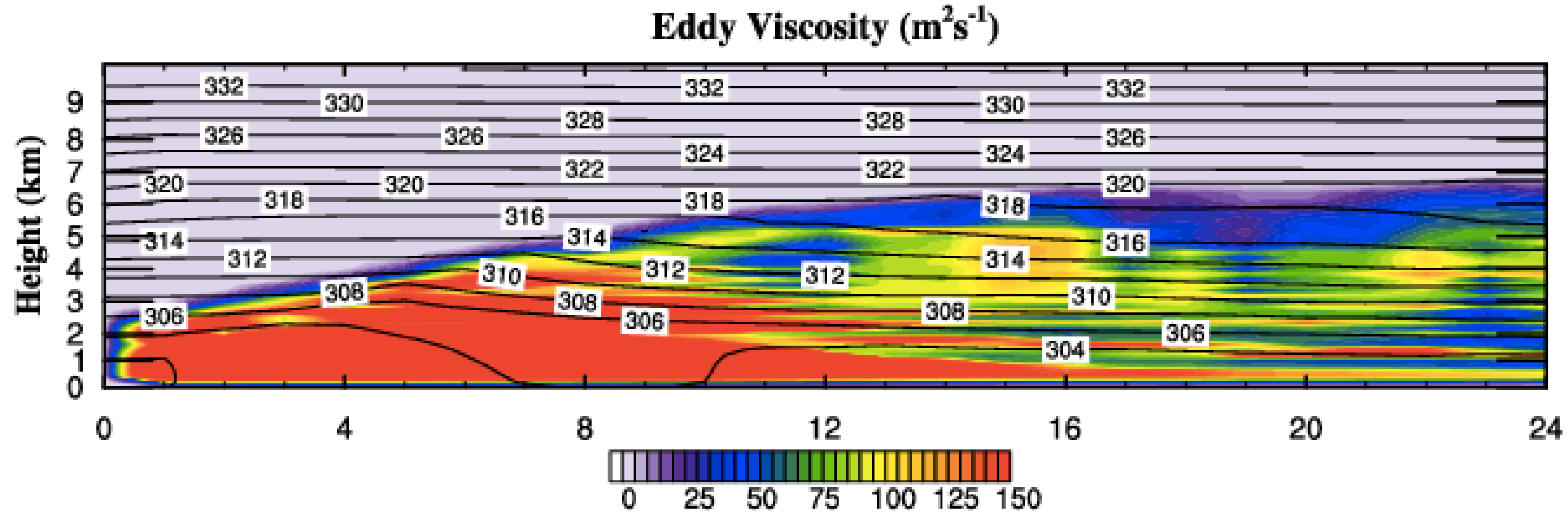


Stress Test: Hurricane SCM case

- TKE-based PBLH develops quickly and extends up to ~5 km
- MYNN SGS clouds do not initiate earlier, but thicken the clouds after hr 12
- SGS cloud mixing ratios tend to be similar to or slightly larger than the resolved-scale mixing ratios



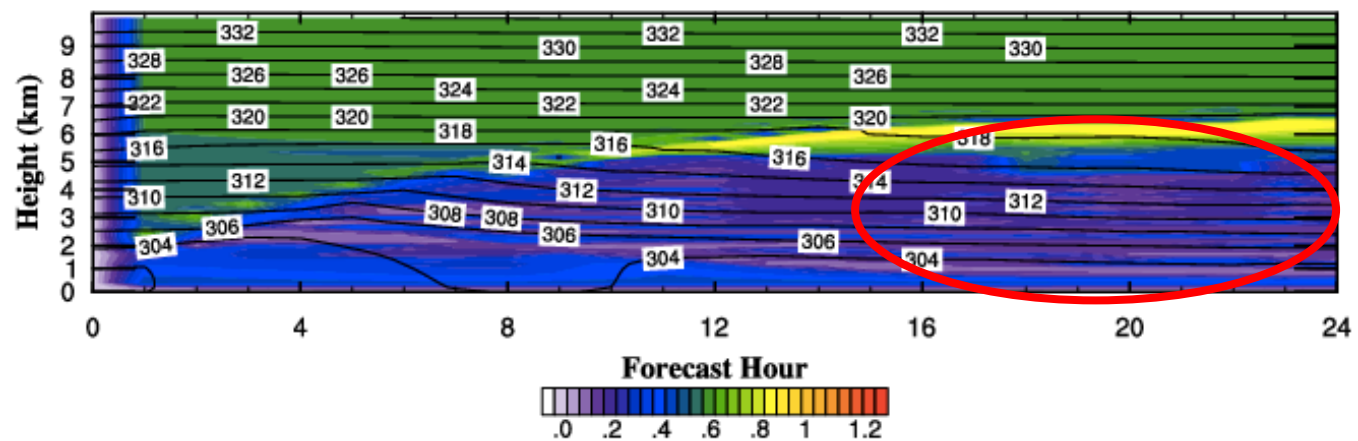
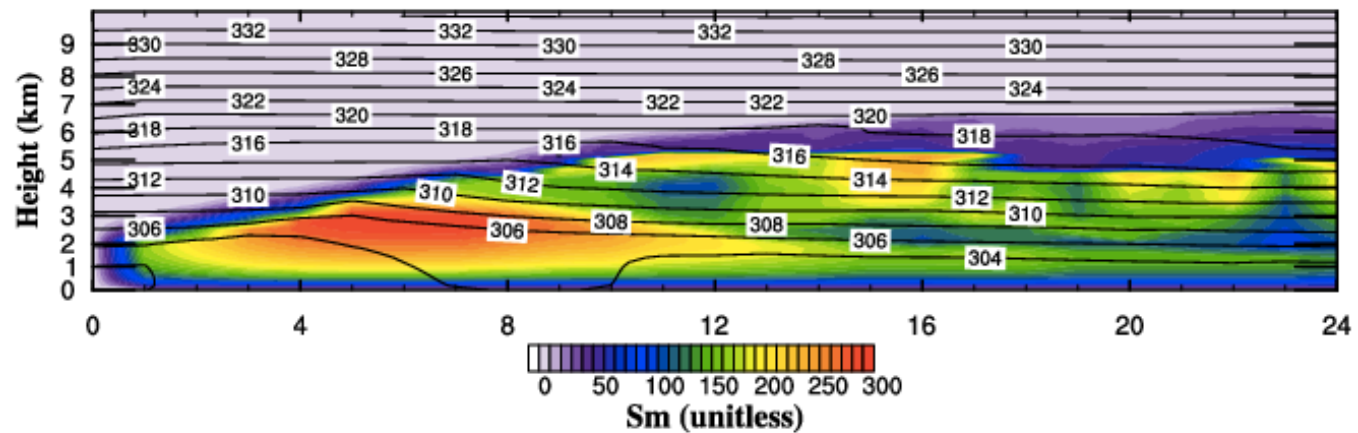
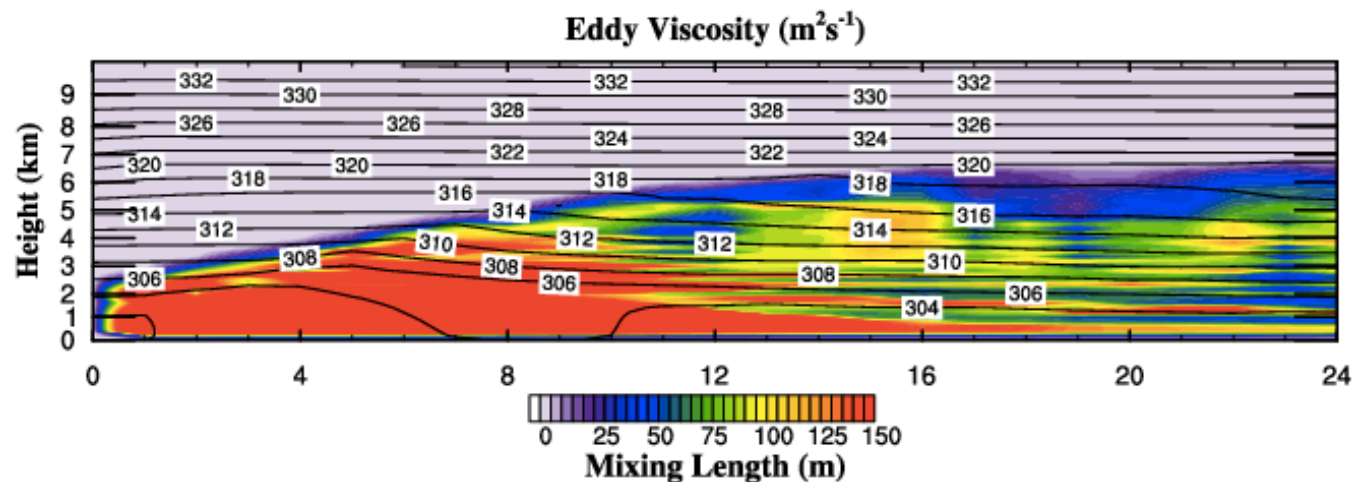
The Problem: Noisy Eddy Viscosity Profiles



$$K_M = q l_m S_M = \text{SQRT}(\text{TKE}) l_m S_M$$

Mixing length

Stability function



The Cause:

The Mellor-Yamada framework uses different stability functions for each closure level, making use of prognostic variables at each level.

The use of two different forms of stability functions in growing ($q_{2.5}/q_{eq} < 1$) and decaying ($q_{2.5}/q_{eq} > 1$) turbulence regimes, where $q_{2.5}$ is the prognosed TKE and q_{eq} is level 2.0 “equilibrium” TKE.

Note: Even when running at level 2.5, the level 2.0 stability functions were used in the growing turbulence regime.

Possible Fixes:

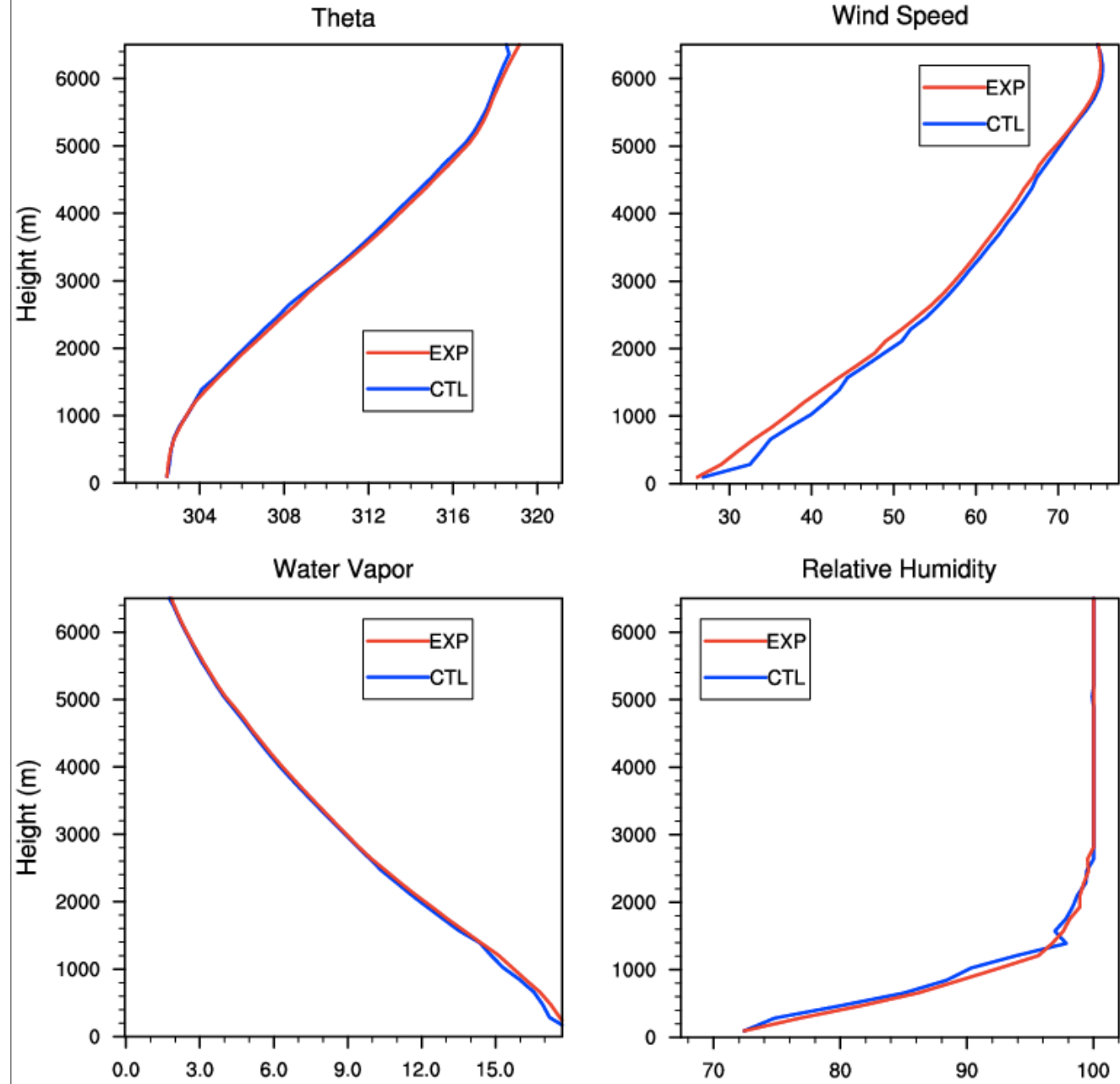
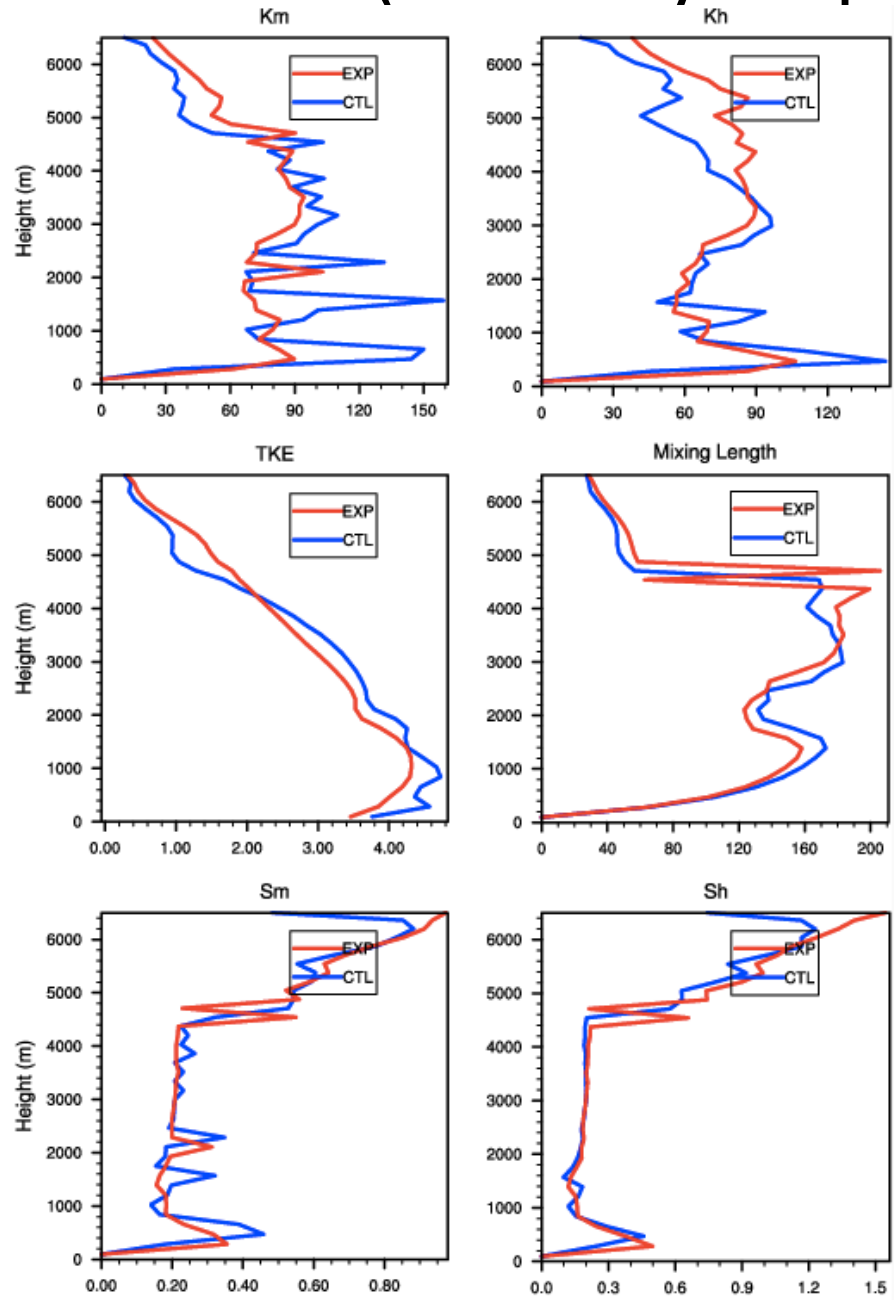
- 1) Use only the level 2.5 forms of S_M and S_H for all regimes.
- 2) ~~Use only the level 2.0 forms of S_M and S_H for all regimes.~~

Using only the level 2.5 stability functions

Note: It was necessary to add additional constraints from Helfand and Labraga (1988) to achieve a computationally stable version.

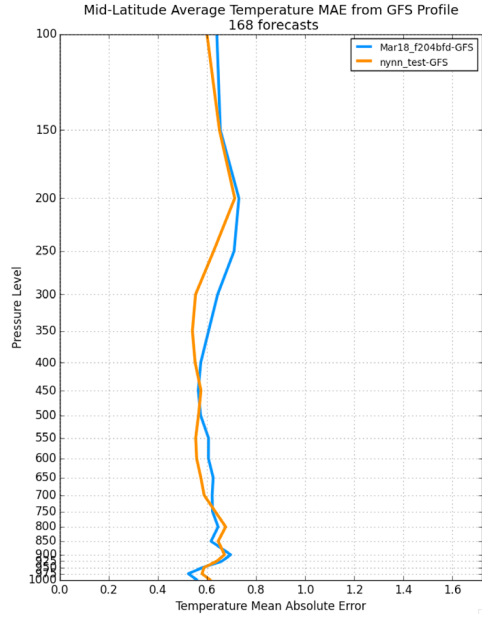
- This suggests that the original coding was intended as so.
- Consequence: when the limits are hit for either (or both) S_M and S_H , the Prandtl number ($Pr = K_M/K_H = S_M/S_H$) can be regulated by the limits.

Hr 18 (mostly equilibrated)

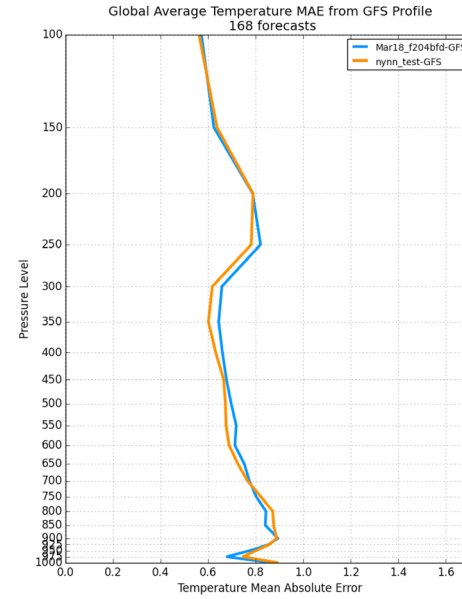


Regionally Averaged Temperature Error Profiles

Mid-Latitude
MAE

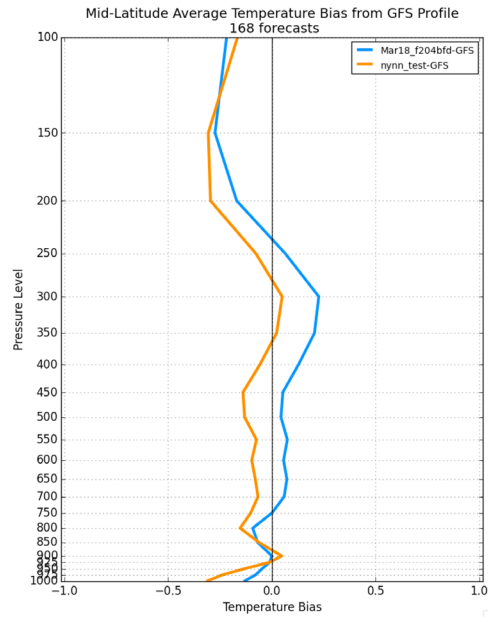


Global MAE

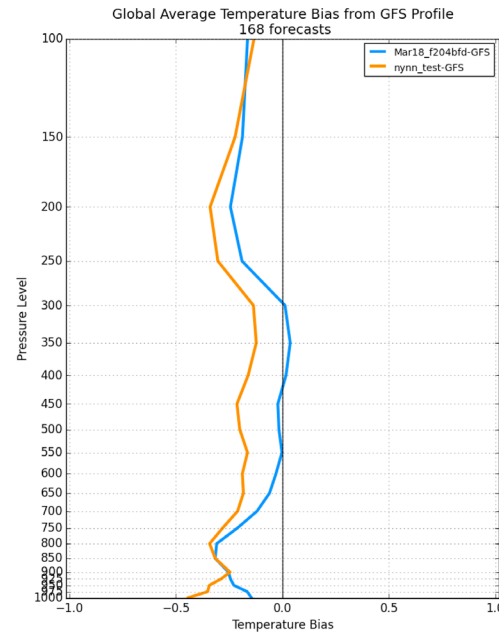


Control
Updated MYNN

Mid-Latitude
Bias



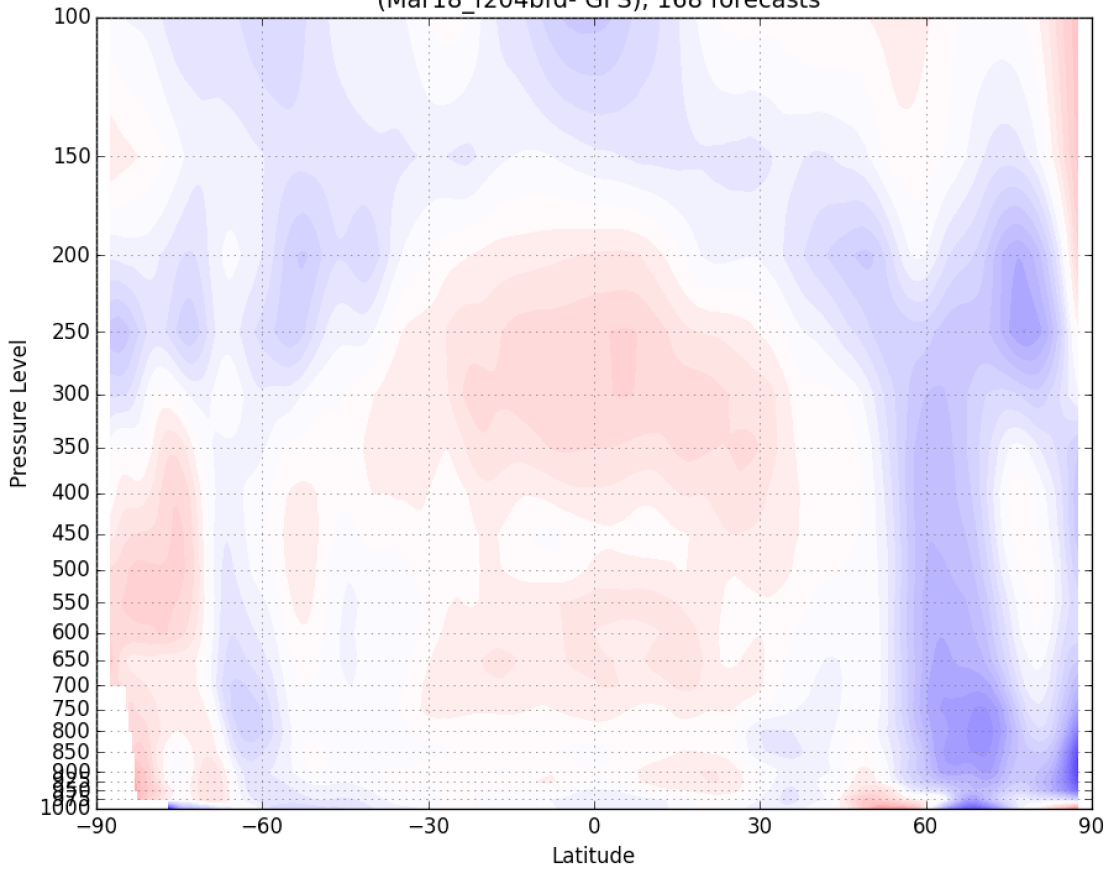
Global Bias



Zonal Temperature Diffs (against GFS analyses)

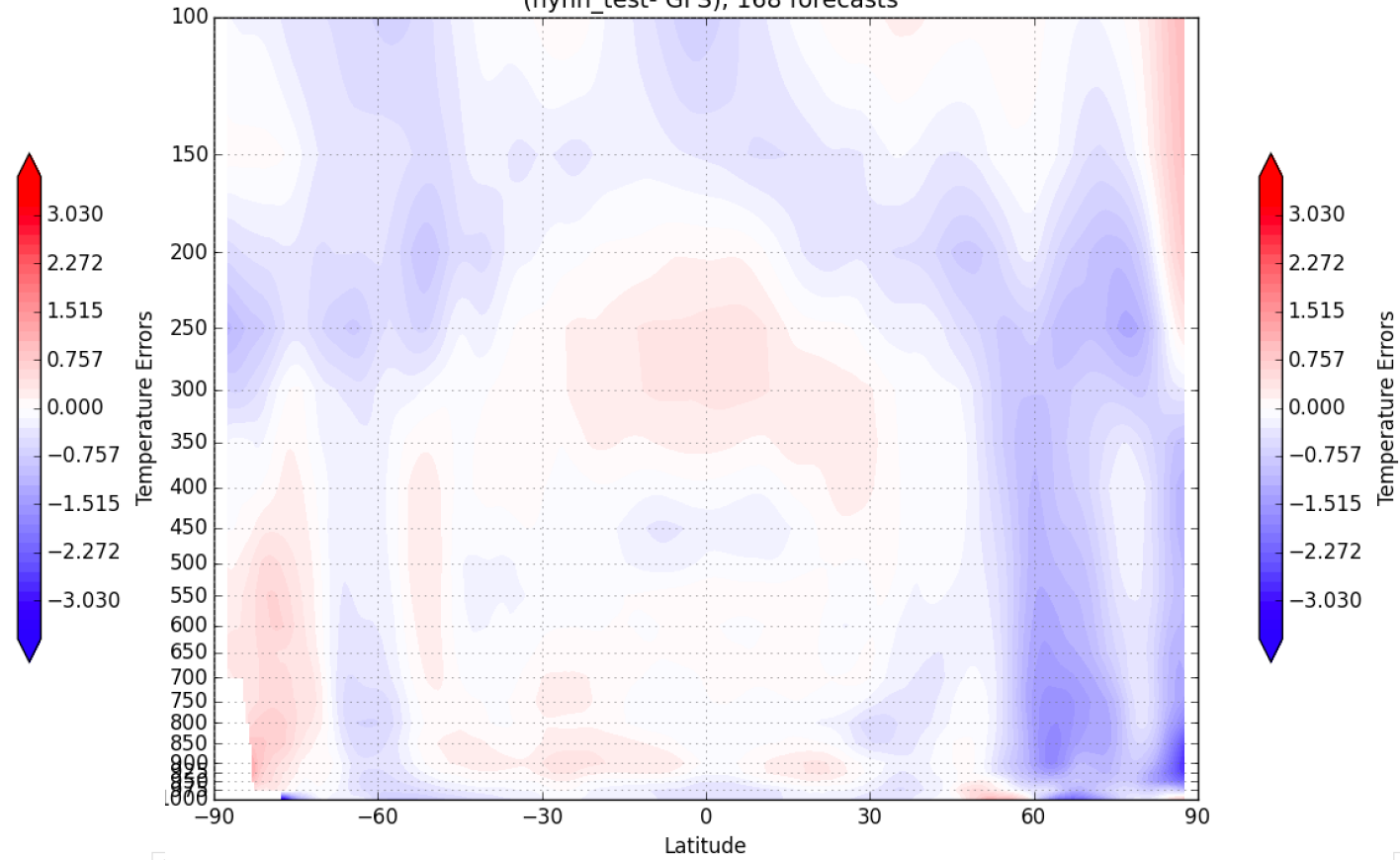
Control

Zonal Contours of Temperature Differences
(Mar18_f204bfd- GFS), 168 forecasts



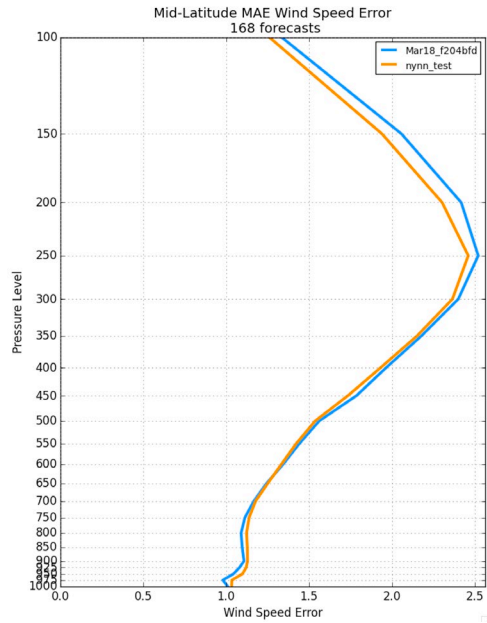
Updated MYNN

Zonal Contours of Temperature Differences
(hynn_test- GFS), 168 forecasts

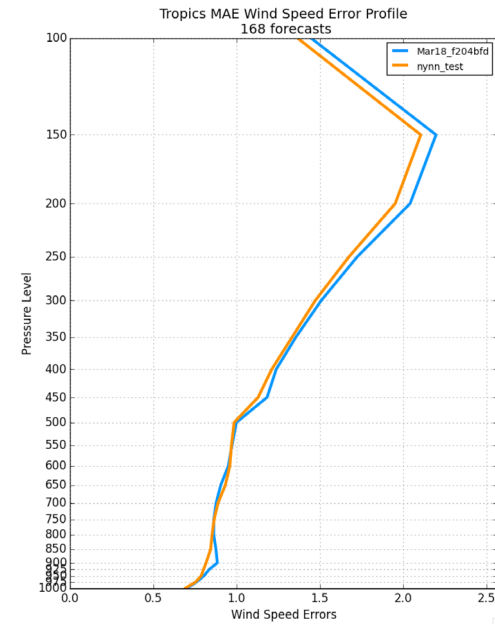


Regionally Averaged Wind Error Profiles

Mid-Latitude
MAE

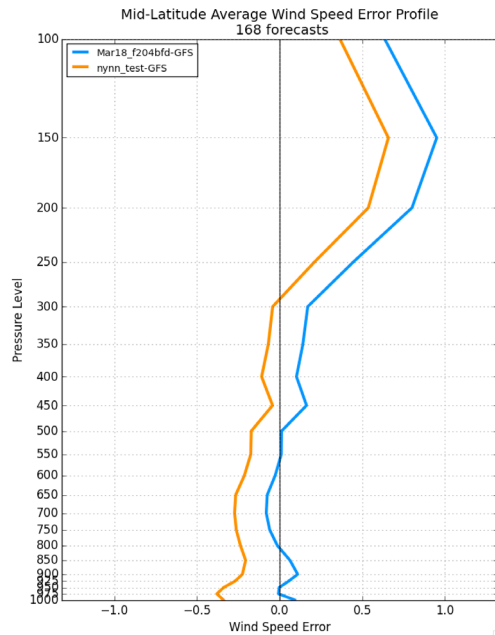


Tropics MAE

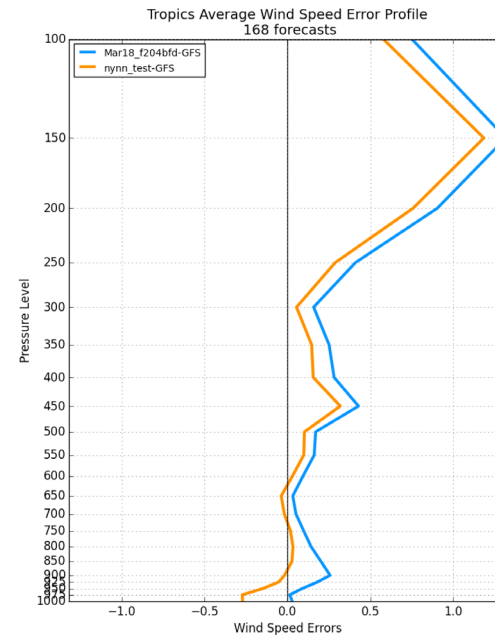


Control
Updated MYNN

Mid-Latitude
Bias



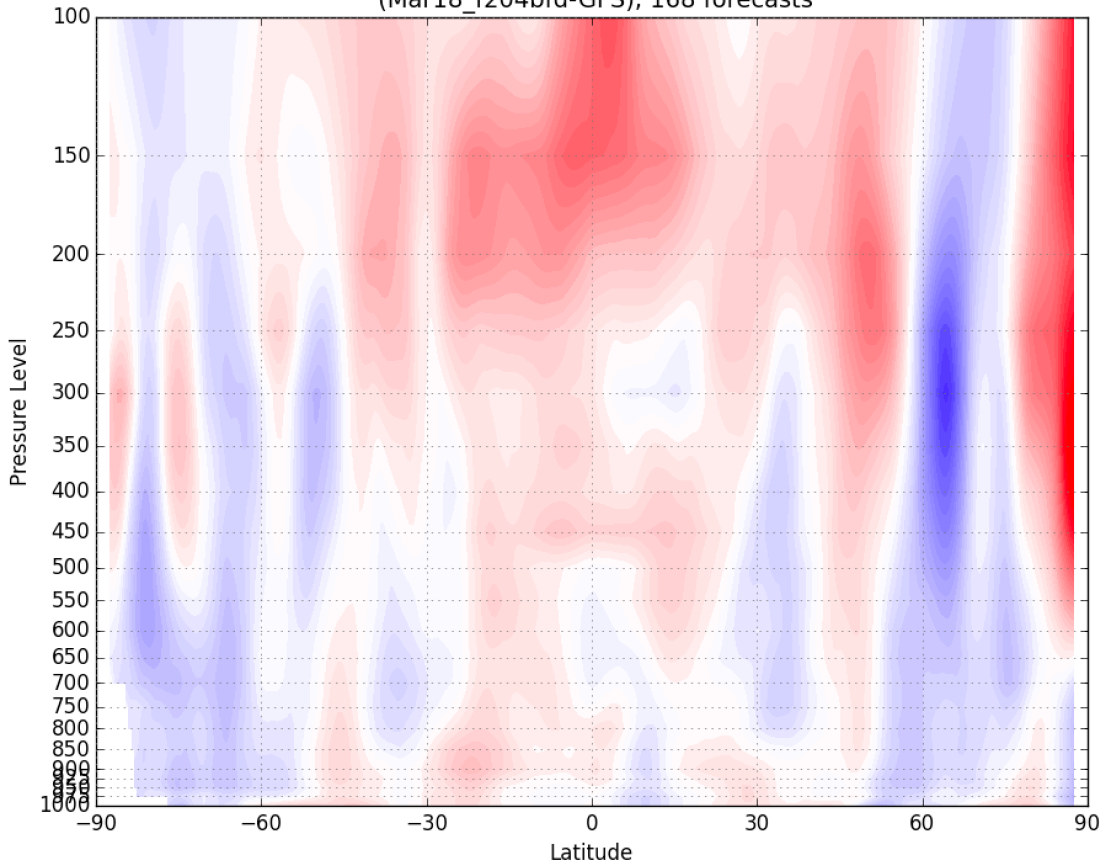
Tropics Bias



Zonal Mean Wind Speed Differences (against GFS Analysis)

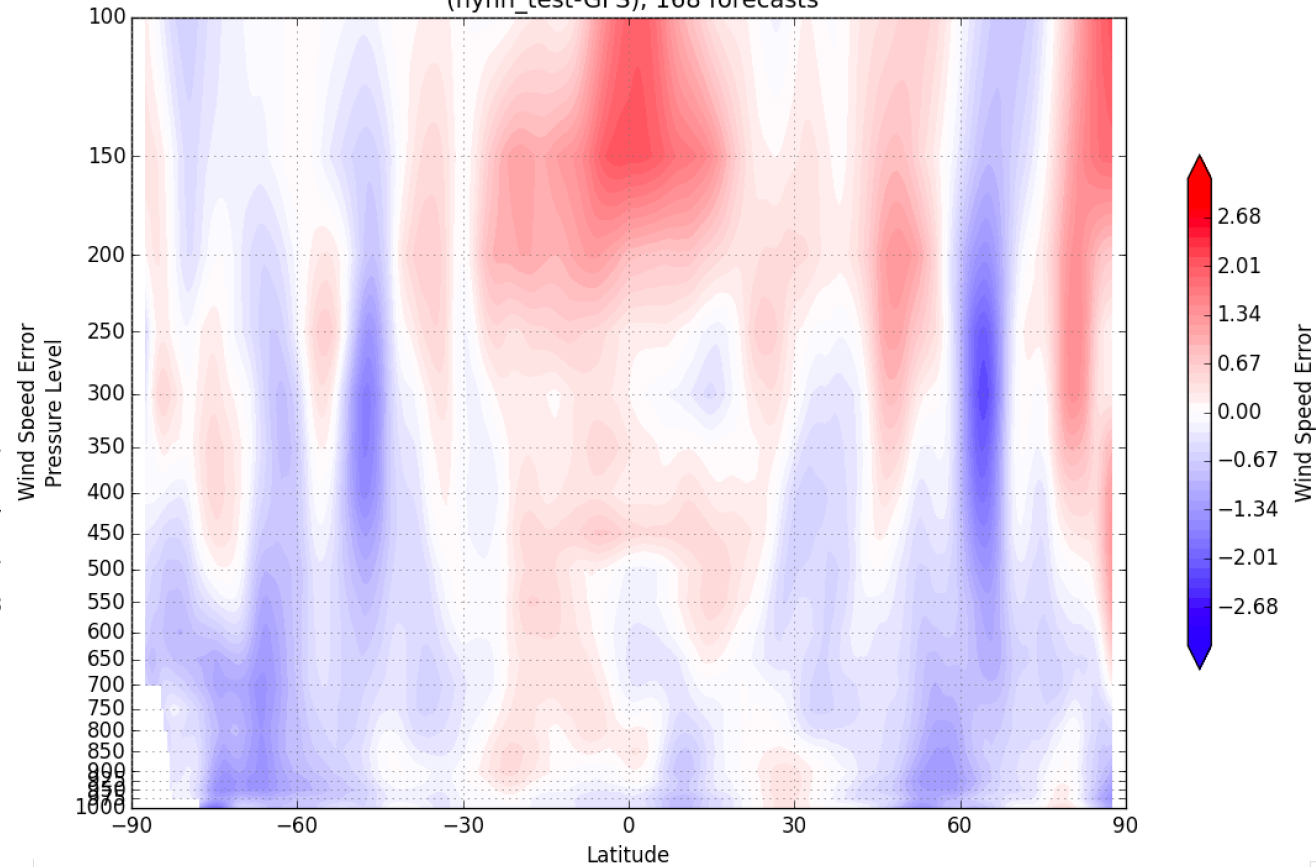
Control

Zonal Contours of Wind Speed Errors
(Mar18_f204bfd-GFS), 168 forecasts



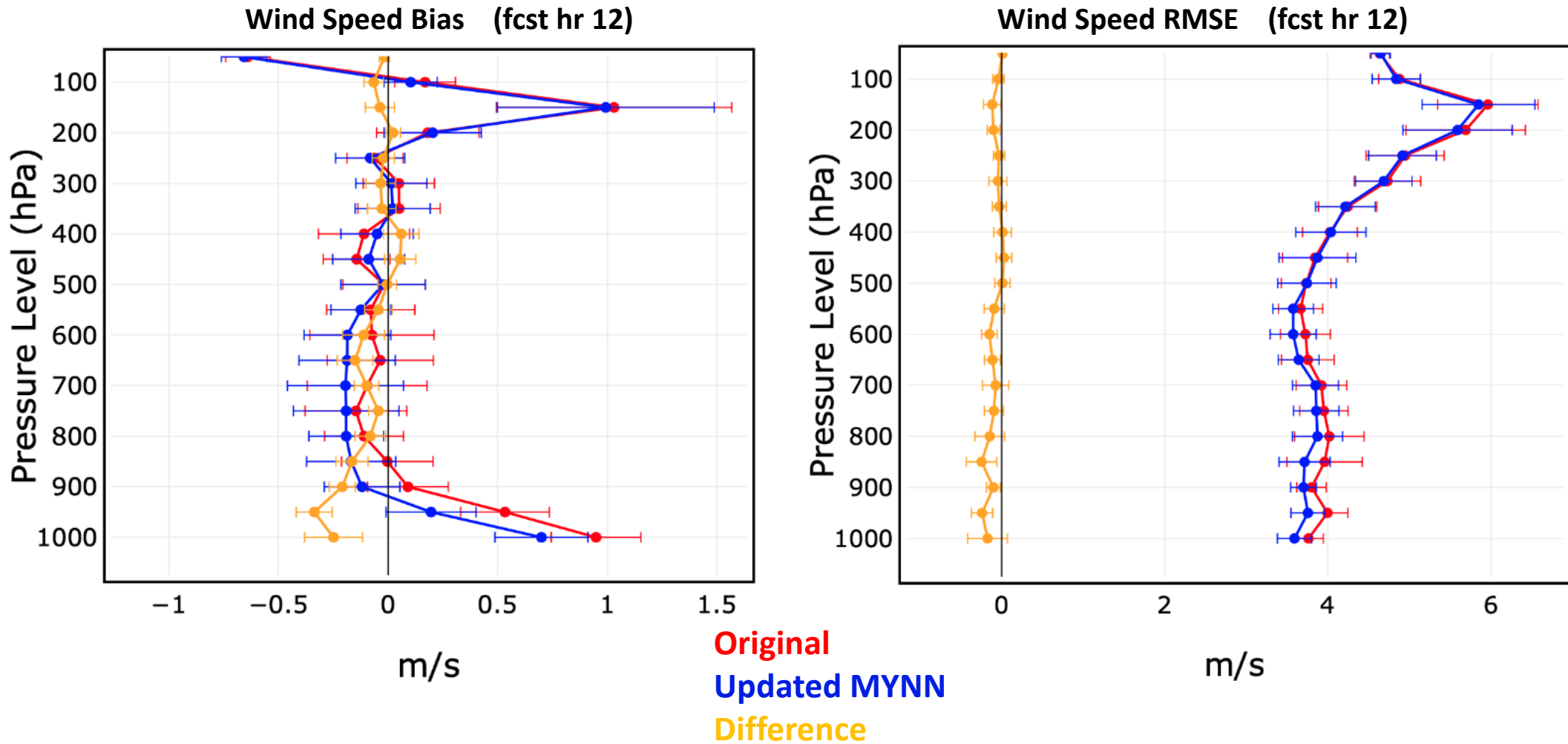
Updated MYNN

Zonal Contours of Wind Speed Errors
(nynn_test-GFS), 168 forecasts



Results from a RRFS Retro (4 -11 Sept 2020):

CONUS composite stats against radiosonde



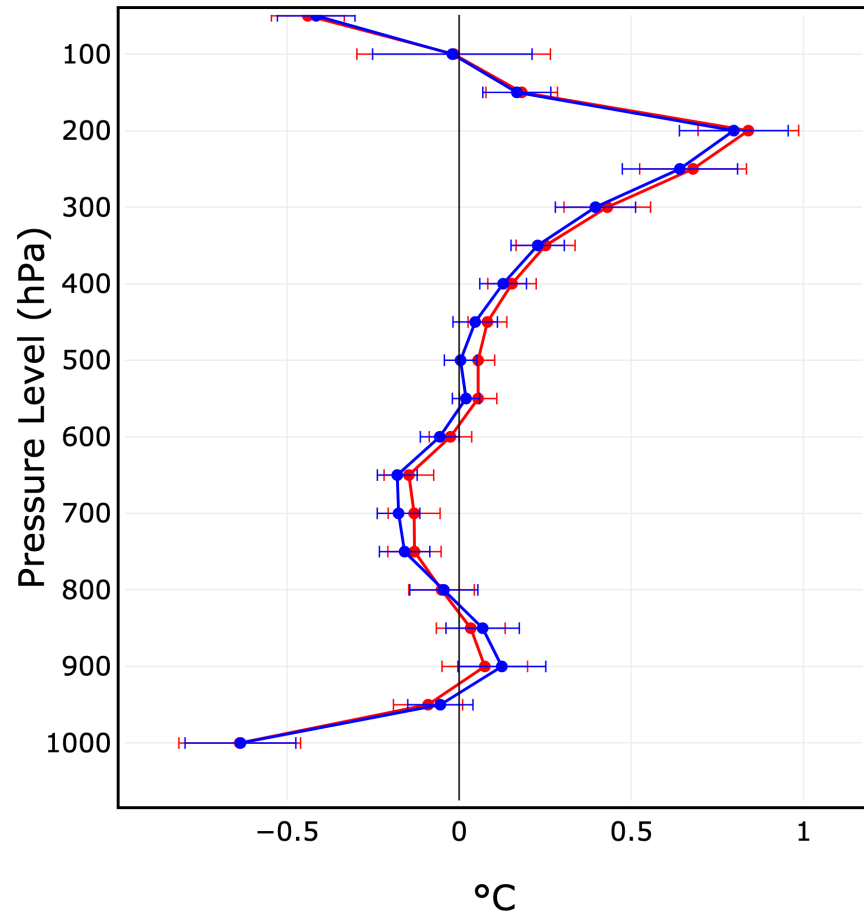
More Results from a RRFS Retro (4 -11 Sept 2020):

CONUS composite stats against radiosonde

Temperature Bias (fcst hr 12)

Upper Air (RAOBS) : Profile: no diffs MATCHED

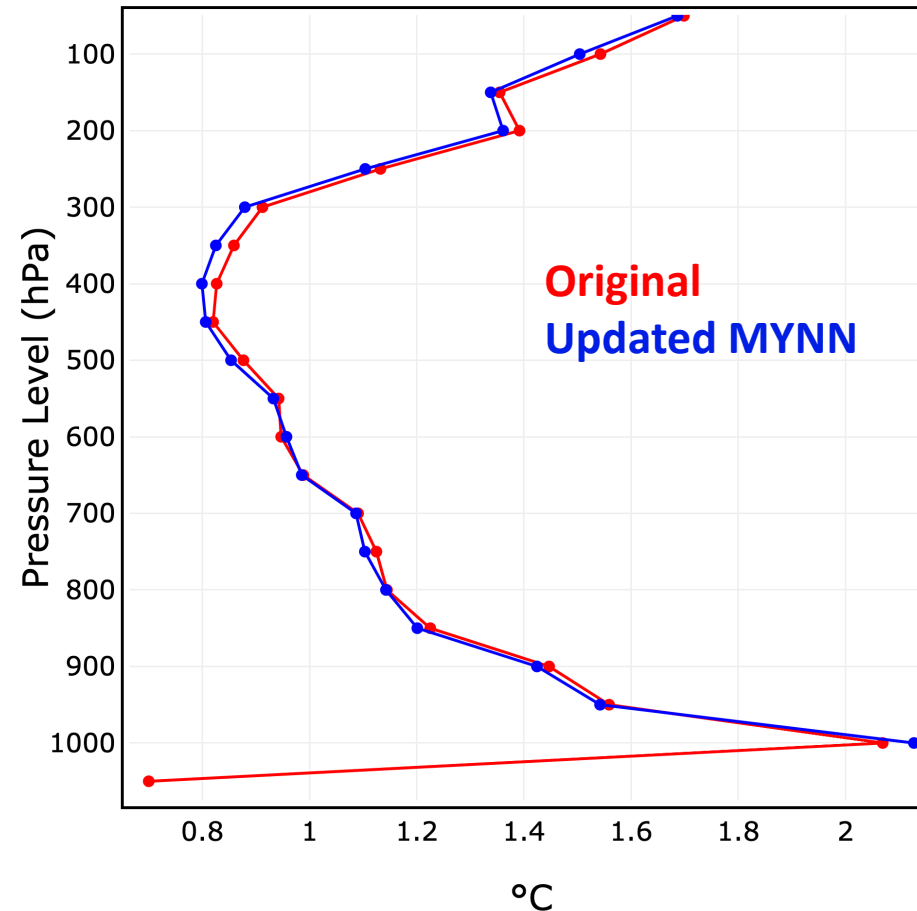
Curve0 mean = 0.05858, median = 0.04439, stdev = 0.3231
Curve1 mean = 0.04412, median = 0.01212, stdev = 0.3127



Temperature RMSE (fcst hr 12)

Upper Air (RAOBS) : Profile: no diffs UNMATCHED

Curve0 mean = 1.174, median = 1.125, stdev = 0.3378
Curve1 mean = 1.183, median = 1.104, stdev = 0.3381



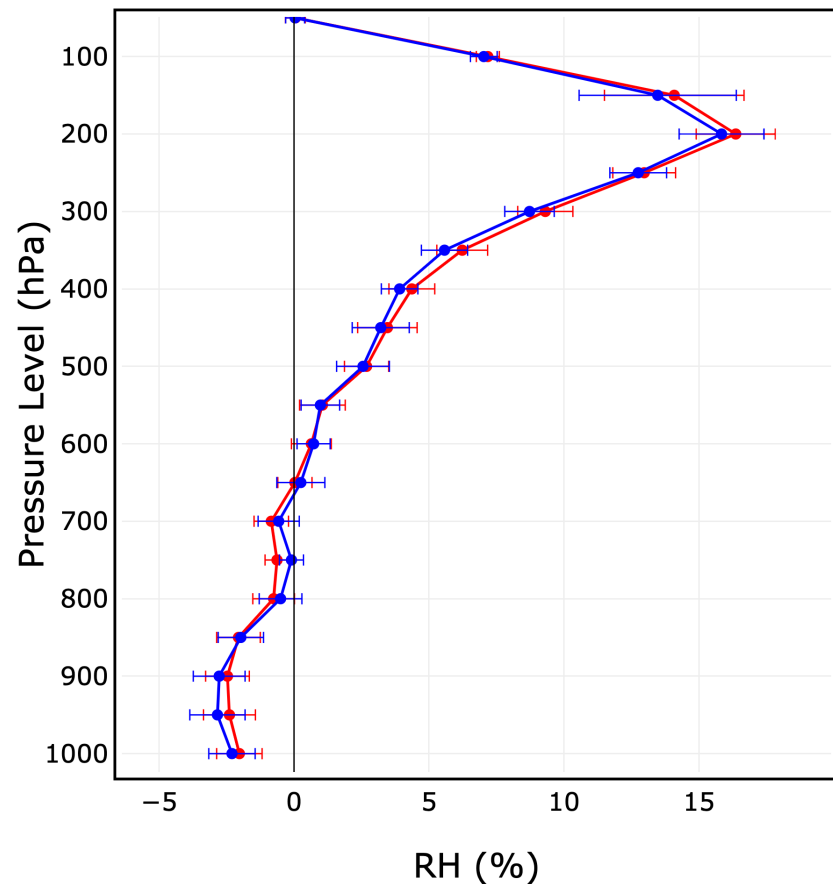
More Results from a RRFS Retro (4 -11 Sept 2020):

CONUS composite stats against radiosonde

RH(obT) Bias (fcst hr 12)

Upper Air (RAOBS) : Profile: no diffs MATCHED

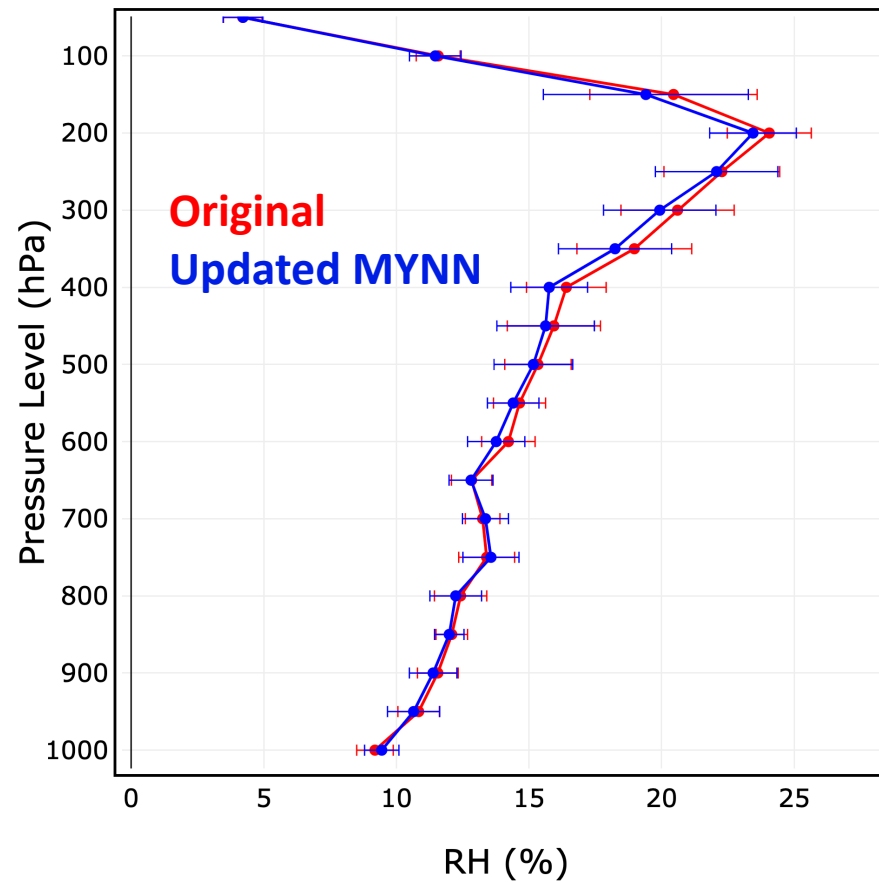
Curve0 mean = 3.363, median = 0.8471, stdev = 5.688
Curve1 mean = 3.201, median = 0.8510, stdev = 5.504

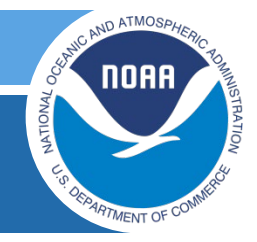
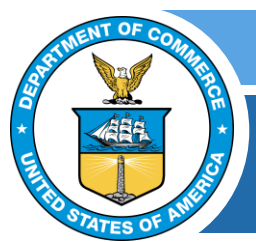


RH(obT) RMSE (fcst hr 12)

Upper Air (RAOBS) : Profile: no diffs MATCHED

Curve0 mean = 14.72, median = 13.82, stdev = 4.639
Curve1 mean = 14.45, median = 13.67, stdev = 4.417



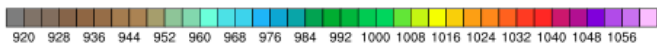
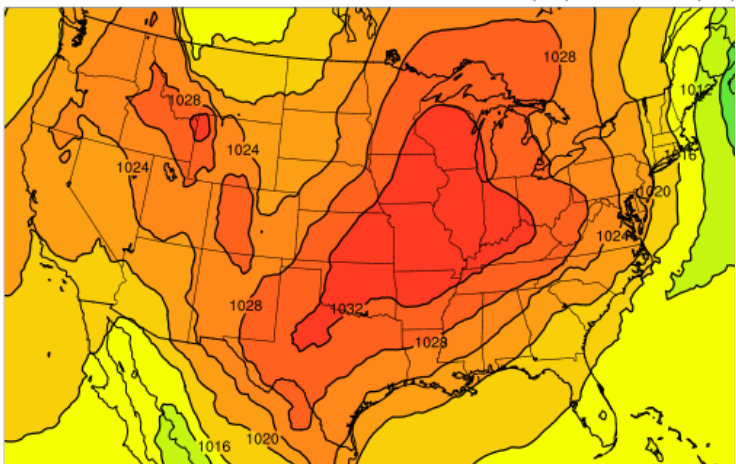


Radiational Cooling Case

Performed by
Alexei Belochitski

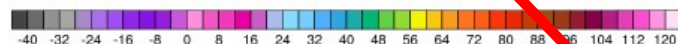
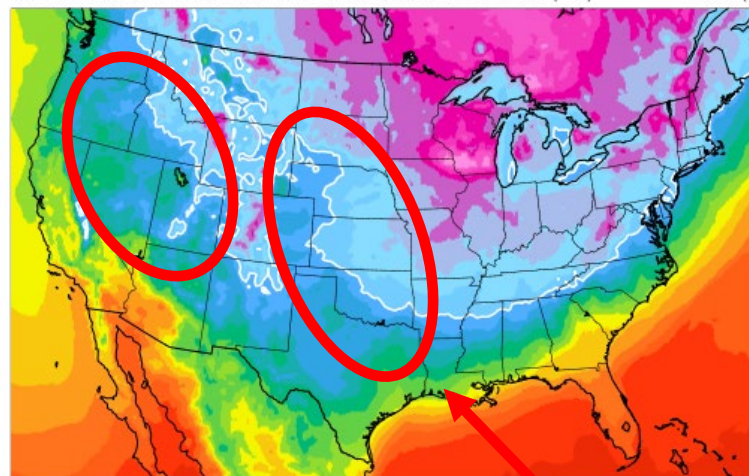
GFSv16 fcst init. 00Z 08 November 2019 valid 12Z 08 November 2019 (F12)

SLP (hPa)



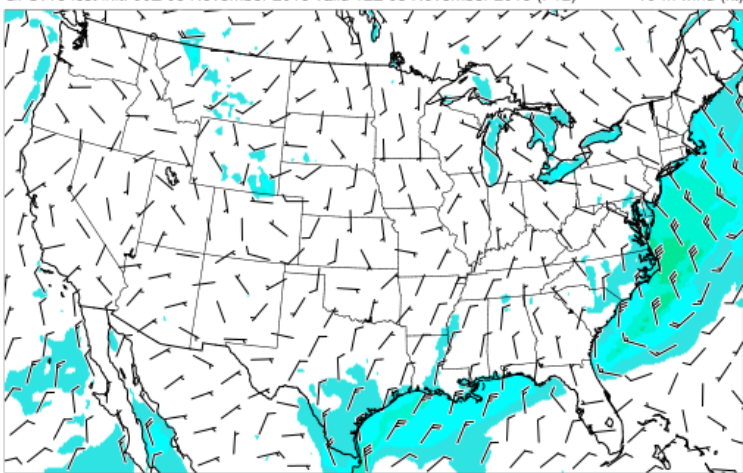
GFSv16 fcst init. 00Z 08 November 2019 valid 12Z 08 November 2019 (F12)

2-m T (F)



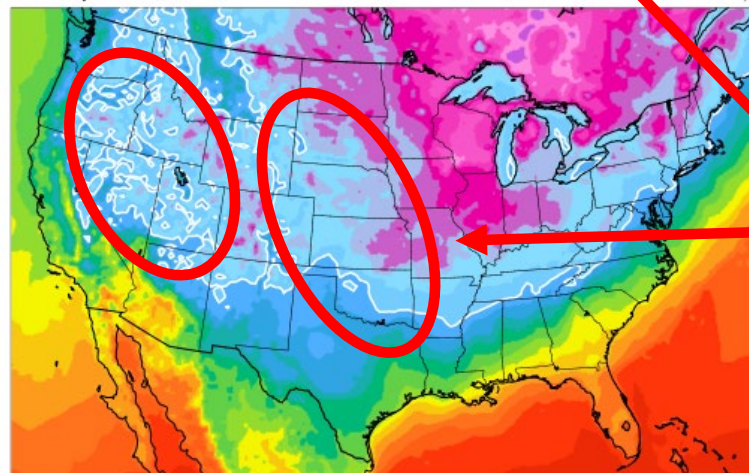
GFSv16 fcst init. 00Z 08 November 2019 valid 12Z 08 November 2019 (F12)

10-m wind (kt)



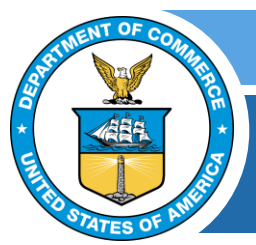
RAP analysis valid 12Z 08 November 2019

2-m T (F)



Valid: 12Z 8 November 2020

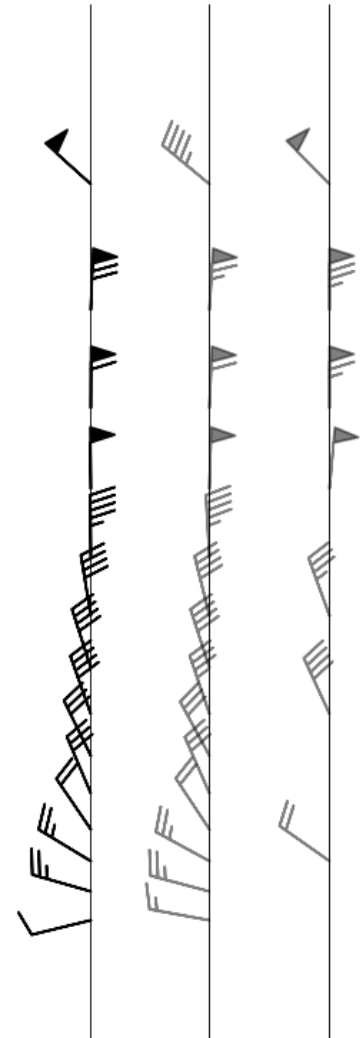
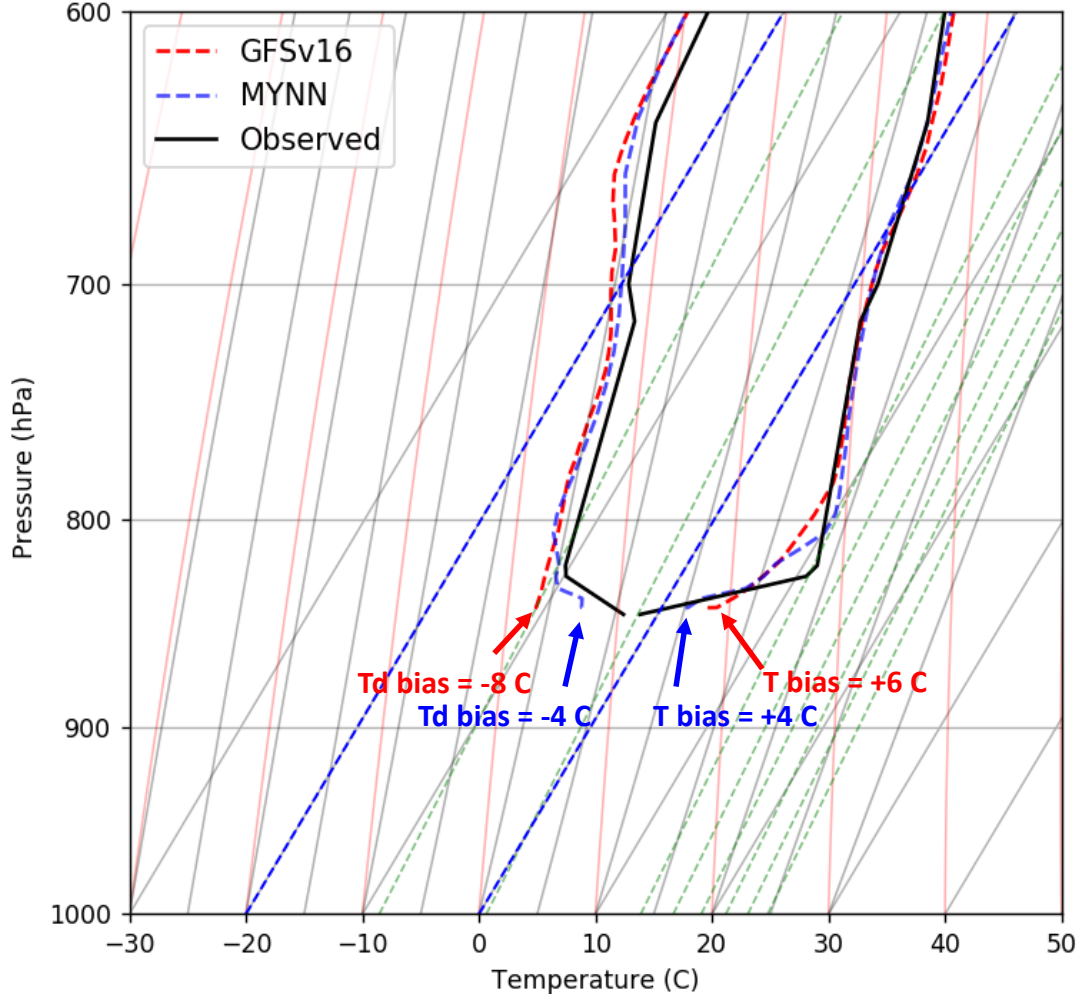
- Relaxed pressure gradient across much of Midwest, Plains, and western U.S., implying very light winds and likely overnight decoupling
- 10m wind field (lower right) and cloud fields (not shown) indicate ideal conditions for radiation inversions and strong cooling over much of the U.S.
- Visually comparing analysis (lower right) to GFSv16 (upper right) clearly shows it's too warm over much of the Midwest, Northern Plains, and the Intermountain West



GFSv16 Temperatures

Performed by
Alexei Belochitski

CCEE01 and ccppC768 vs. Observed at KDNR
Forecast Hour 12
Init: 00 UTC 08 Nov 2019
Valid: 12 UTC 08 Nov 2019



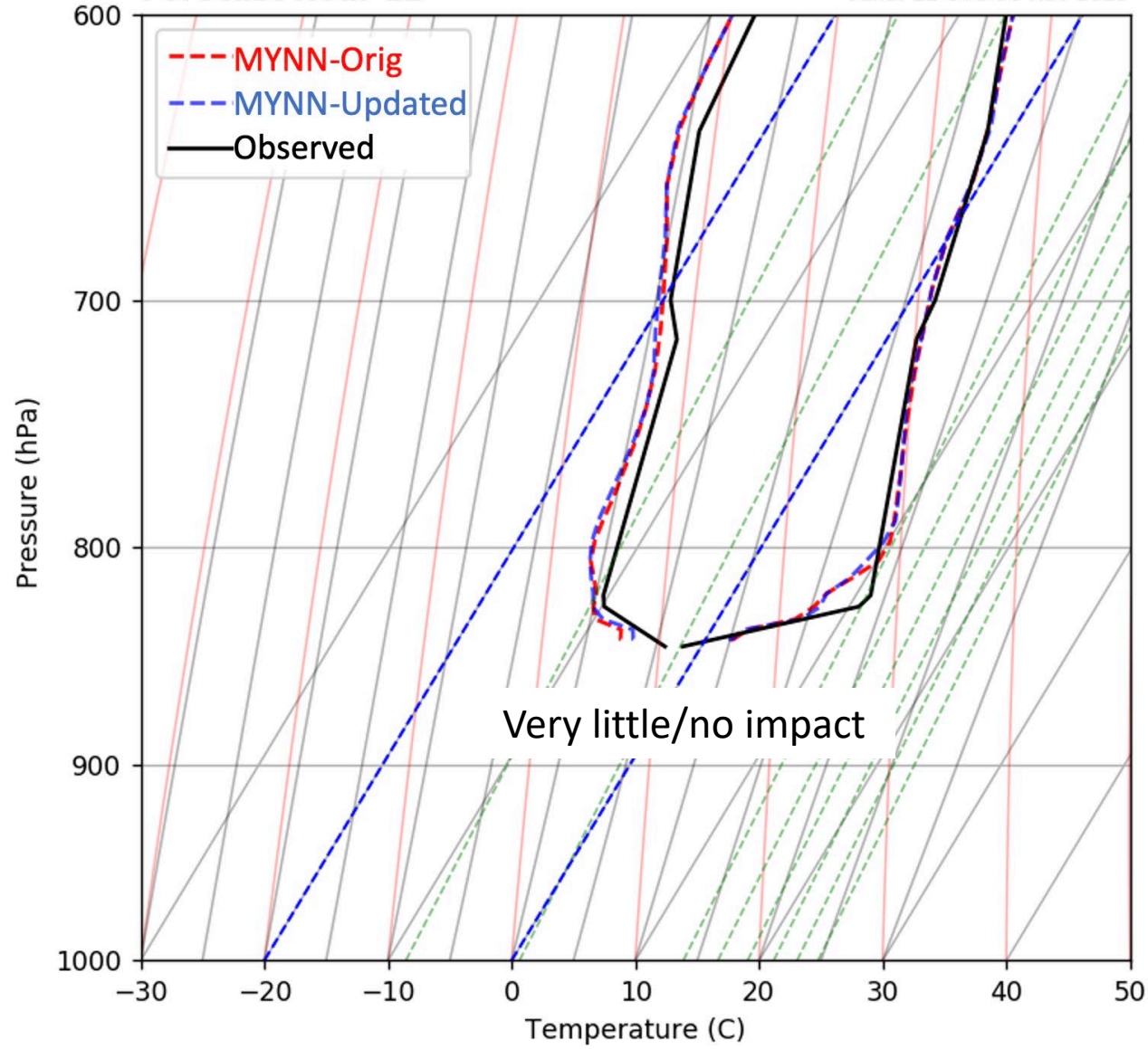
Denver, CO DNR

Init: 00Z 8 November 2019
Valid: 12Z 8 November 2019 (F012)

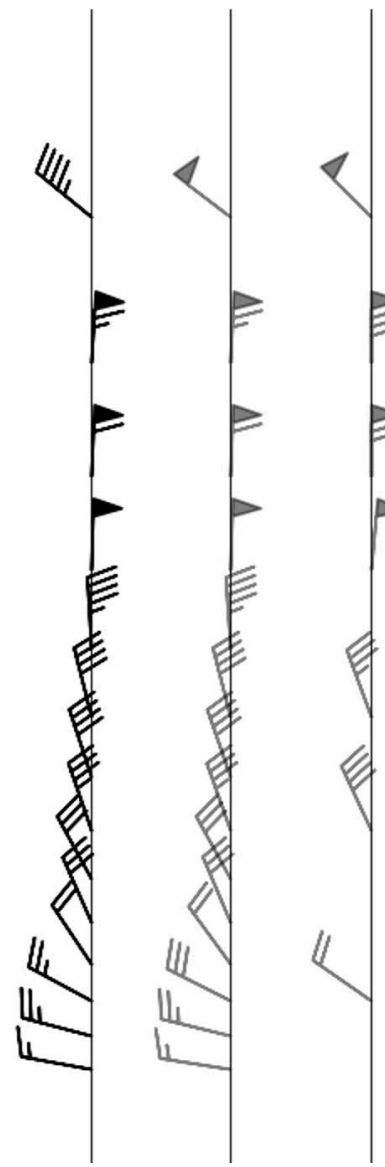
- GFSv16 failed to capture the strength of the low-level inversion and ends up way too warm at the lowest levels
- GFS-MYNN improves the surface temperature and dewpoint, and is warmer than GFS at the inversion top

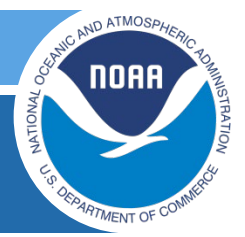
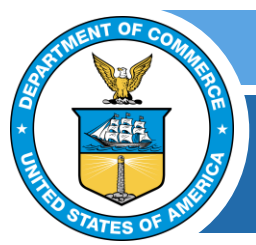
ccppC768 and ccppC768b vs. Observed at KDNB
Forecast Hour 12

Init: 00 UTC 08 Nov 2019
Valid: 12 UTC 08 Nov 2019



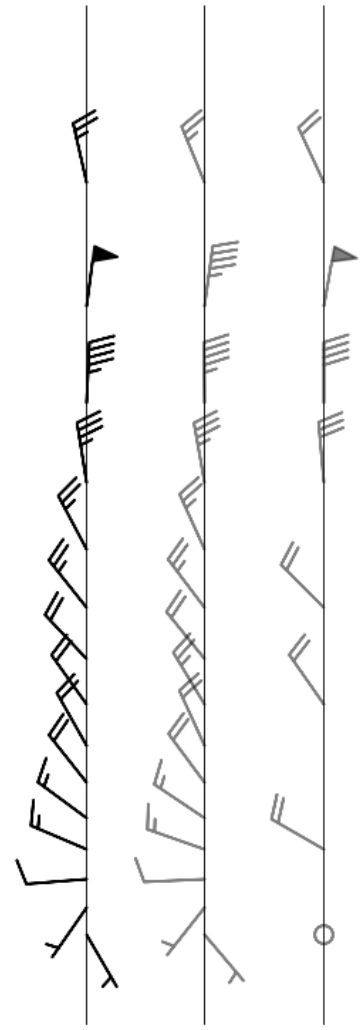
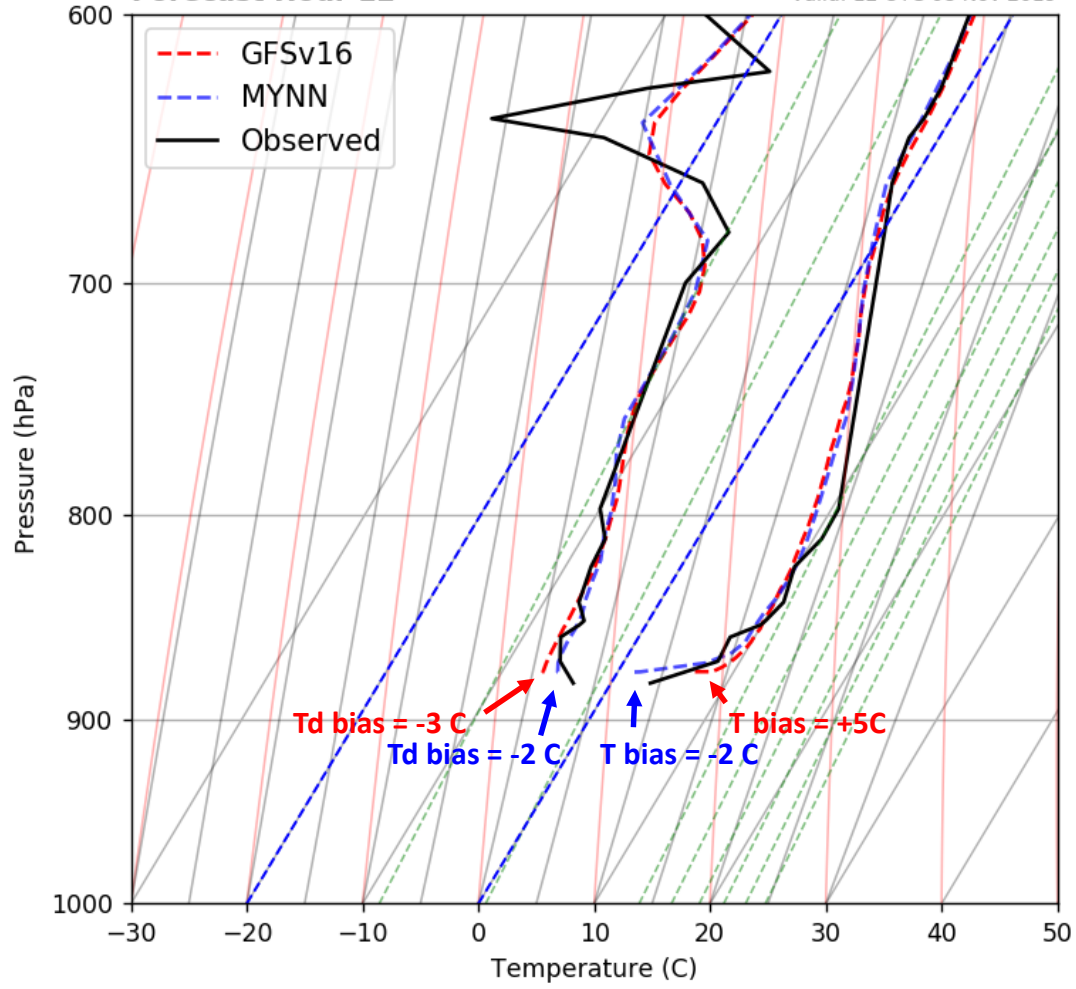
Simulations performed by
Alexei Belochitski





SLC Soundings

CCEE01 and ccppC768 vs. Observed at KSLC Init: 00 UTC 08 Nov 2019
Forecast Hour 12 Valid: 12 UTC 08 Nov 2019



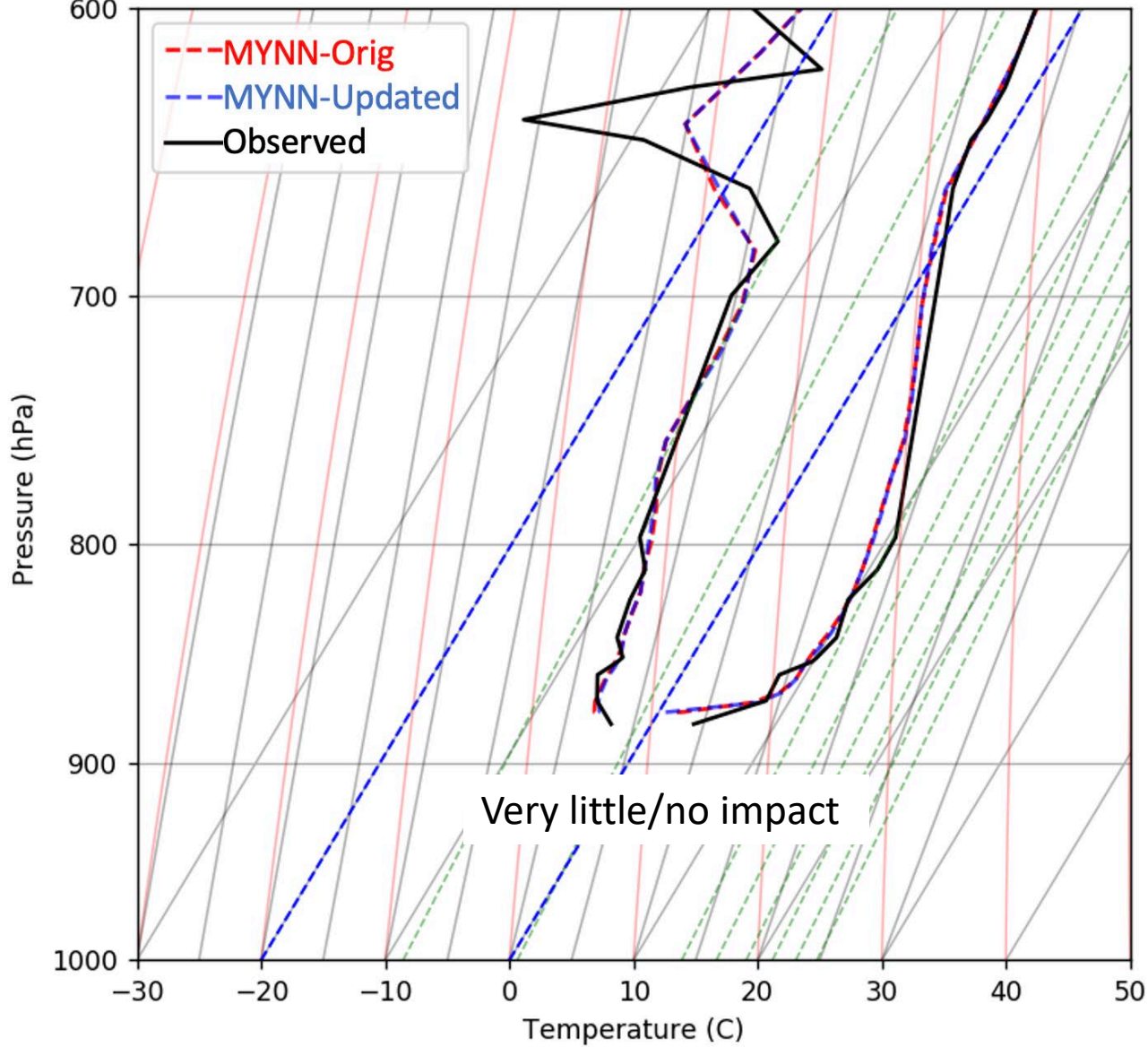
Salt Lake City, UT SLC

Init: 00Z 8 November 2019
Valid: 12Z 8 November 2019 (F012)

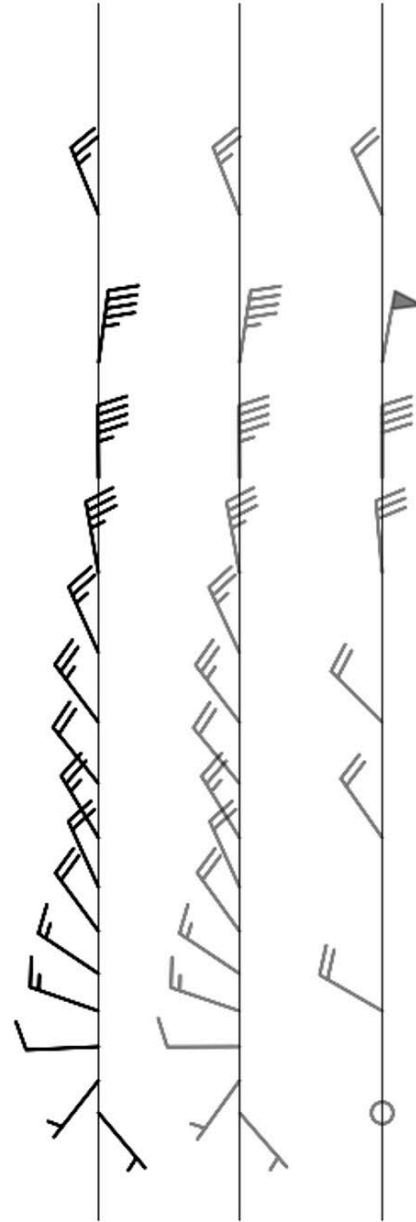
- GFSv16 fails to capture the strength of the low-level inversion and ends up ~5 C too warm at the lowest levels
- GFS-MYNN is colder and moister, but is slightly too cold at the surface.

ccppC768 and ccppC768b vs. Observed at KSLC
Forecast Hour 12

Time: 00 UTC 08 Nov 2019
Valid: 12 UTC 08 Nov 2019



Simulations performed by
Alexei Belochitski



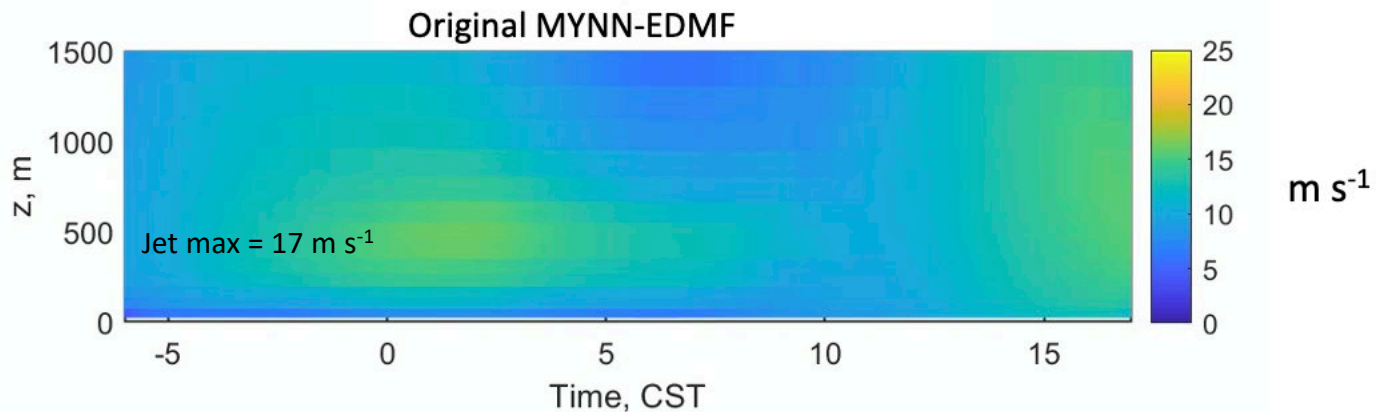
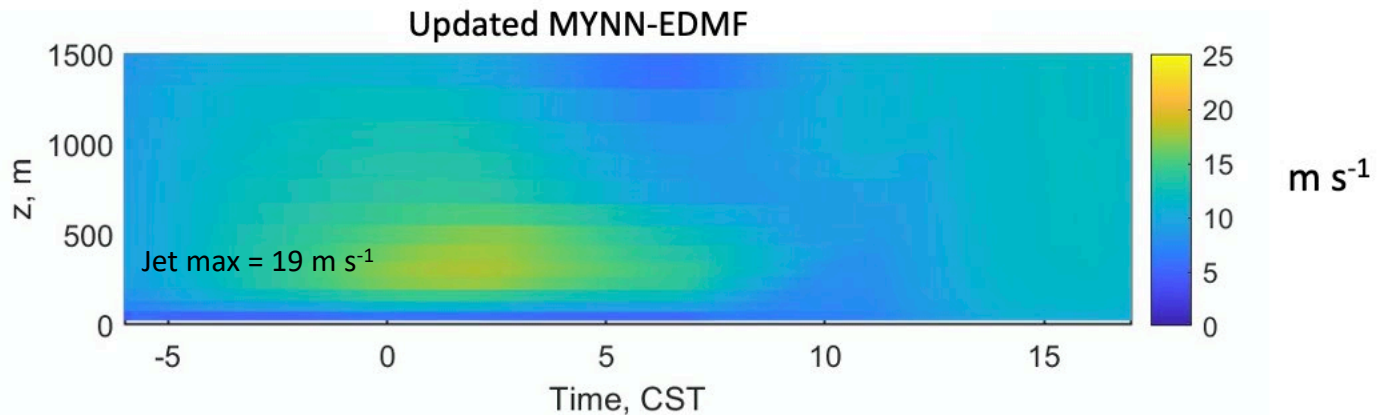
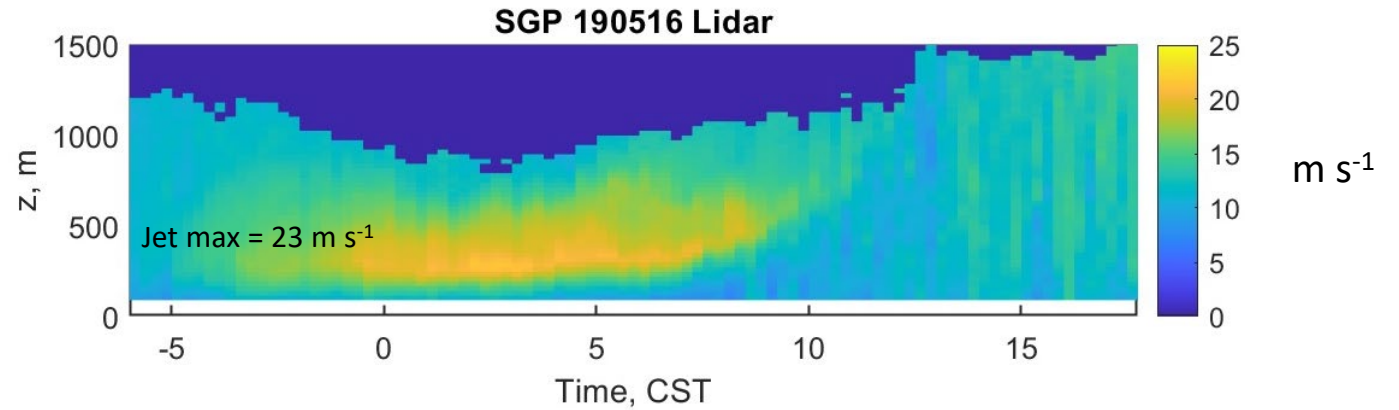
SCM SGP LLJ case

Setup:

- CCPP SCM
- Model top=100 mb
- 51 levels
- timestep: 60 sec

Results:

- Increased jet max
- Jet is still weaker and less sharp than in lidar observations
- Still investigating forcing/vertical resolution



Summary for Work on Numerical Pathologies

- Numerical pathology was diagnosed – stability functions were the cause
 - Switching to the level 2.5 stability functions provides some improvements
 - Concerned about hitting limits – impacting the Prandtl number ($Pr = S_m/Sh$)
 - Further investigation is required
- Impacts seem to improve the wind and temperature profiles
 - Largest improvements are in the upper troposphere
 - Concerned about a negative wind speed bias at low-levels
- Eddy-diffusivity-specific regime testing:
 - Updated stability functions do not adversely impact successful radiational cooling stable-layer cases
 - Low-level jet SCM case was improved

Improving Clouds

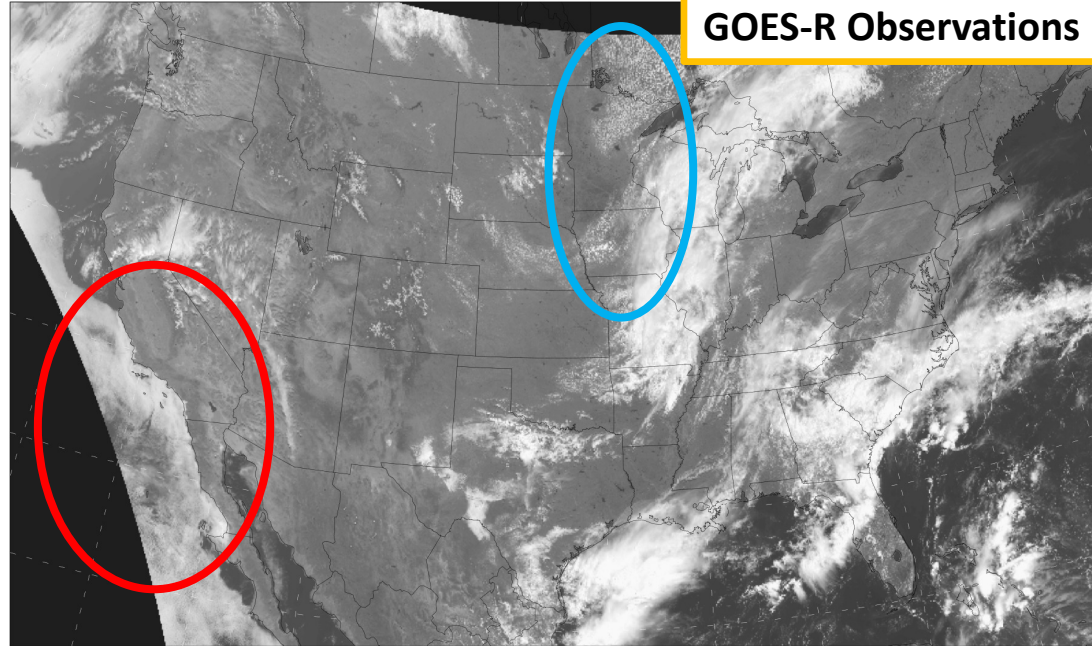
Comparison of SW-up at TOA

Valid: 16 UTC 12 June 2019

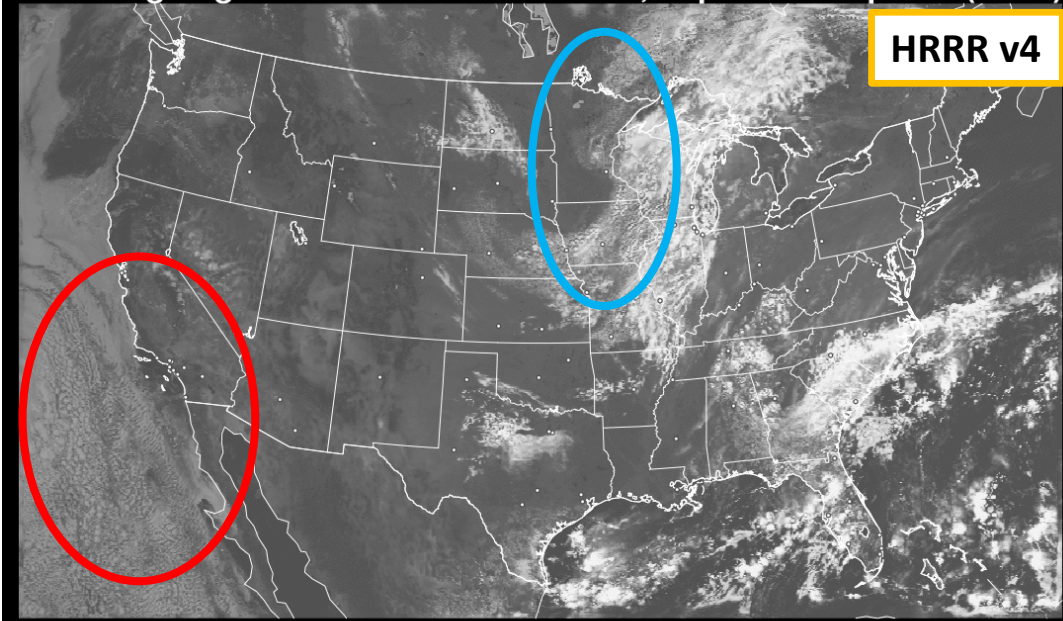
Initialized 06 UTC 11 June
(Forecast hour 34)

GOES-16 combined (ch1, 2, 3) visible albedo

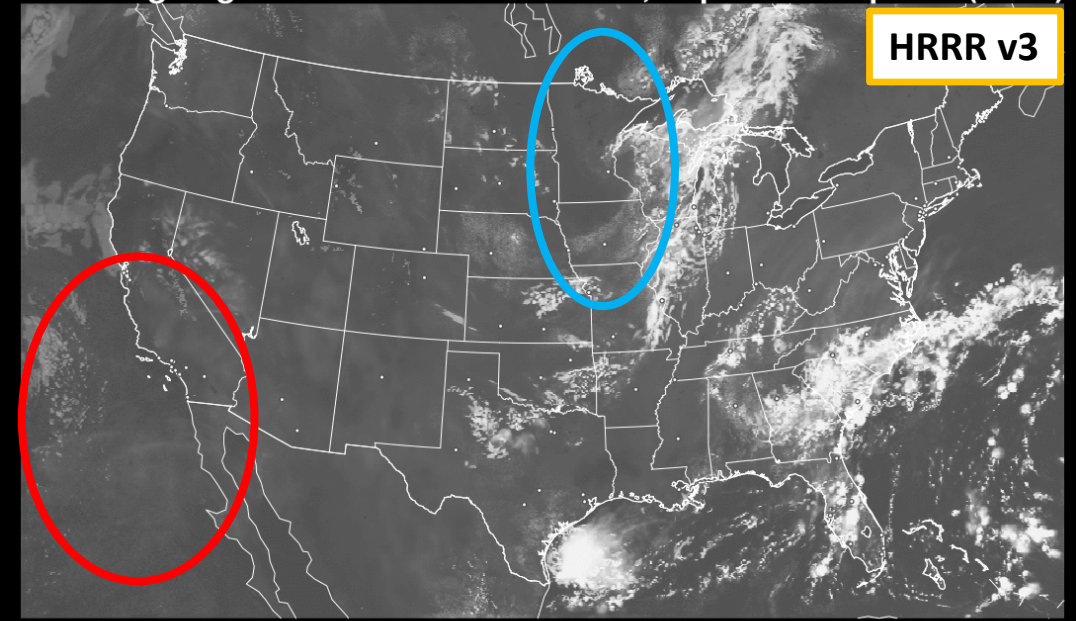
16:03:06 12 Jun 2019



HRRRX 06/11/2019 (06:00) 34h fcst - Experimental
Valid 06/12/2019 16:00 UTC
Outgoing Shortwave Radiation Flux, Top of Atmosphere (W/m^2)

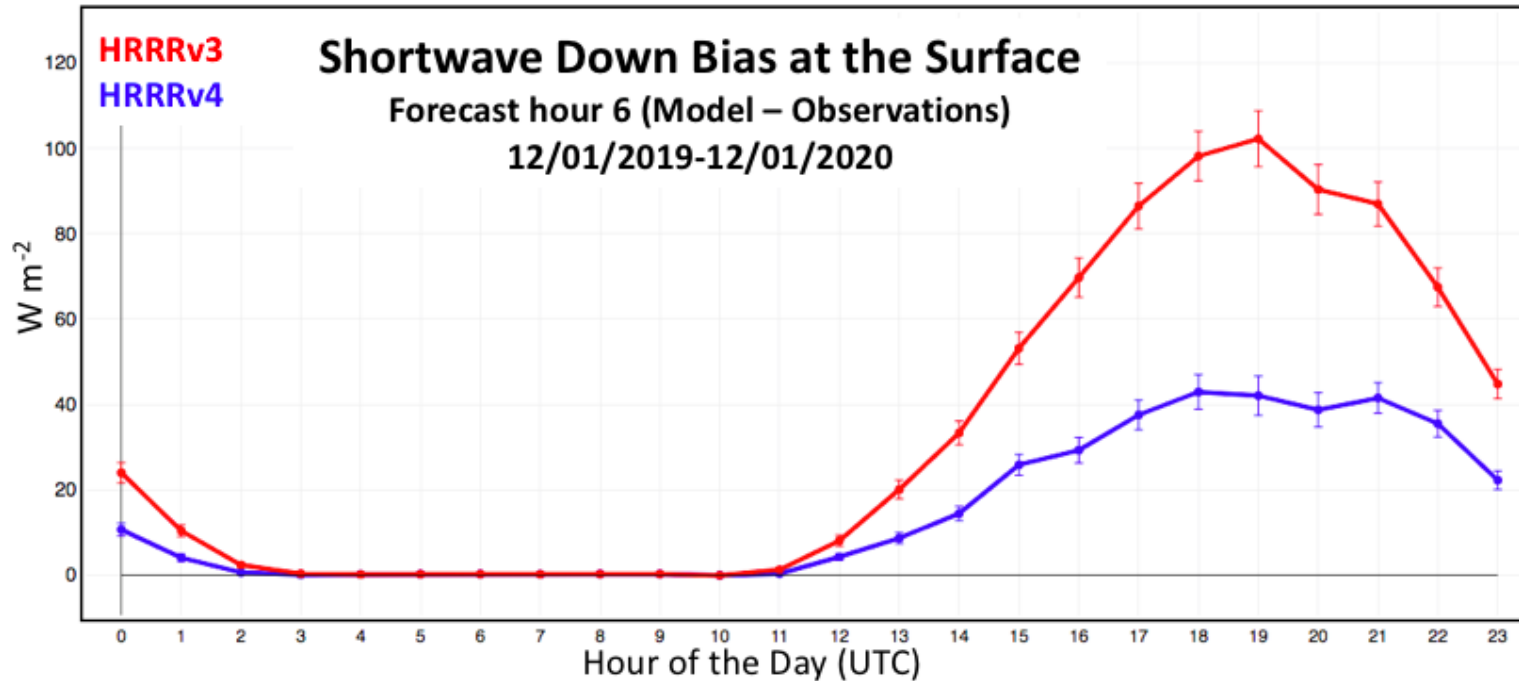


HRRR-NCEP 06/11/2019 (06:00) 34h fcst
Valid 06/12/2019 16:00 UTC
Outgoing Shortwave Radiation Flux, Top of Atmosphere (W/m^2)



50 90 130 170 210 250 290 330 370 410 450 490 530 570 610 650 690 730 770 810 850 50 90 130 170 210 250 290 330 370 410 450 490 530 570 610 650 690 730 770 810 850

Despite improvements, there are still large biases



Comparisons were made to GML's 14 SurfRad/SolRad sites across the CONUS

Aspects to revise/investigate:

- 1) Cloud depth
- 2) Cloud cover
- 3) Mixing ratios (q_c , q_i , q_s , etc)
- 4) Liquid/Ice/Snow water path
- 5) Hydrometeor effective radii
- 6) Cloud overlap
- 7) Diurnal cycle of shallow cumulus, etc...

Recent Development Activities:
Higher-Order Moment
Cloud PDF for Stratus Clouds

Chaboureaux-Bechtold Stratiform Cloud Fraction:

First-Order Form

The subgrid variability of the saturation deficit, s , is expressed in terms of the total water, q_w , and liquid water temperature:

$$\sigma_s = c_\sigma l \left(\bar{a}^2 \left(\frac{\partial \bar{q}_w}{\partial z} \right) - 2\bar{a}\bar{b}C_{pm}^{-1} \frac{\partial \bar{T}_l}{\partial z} \frac{\partial \bar{q}_w}{\partial z} + \bar{b}^2 C_{pm}^{-2} \left(\frac{\partial \bar{T}_l}{\partial z} \right)^2 \right)^{1/2}$$

Where c_σ is a tuning constant, l is the mixing length, and a and b are thermodynamic functions arising from the linearization of the function for the water vapor saturation mixing ratio.

$$\bar{a} = \left(1 + L \frac{\partial q_{sat}(T_l)}{\partial T} / C_{pm} \right)^{-1} \quad \bar{b} = \bar{a} \frac{\partial q_{sat}(T_l)}{\partial T}$$

Normalized saturation deficit: $Q_1 = \bar{a}(\bar{q}_w - q_{sat}(\bar{T}_l))/\sigma_s$

Cloud fraction: $cf = \text{MAX}\{0, \text{MIN}[1, 0.5 + 0.36\text{ATAN}(1.55Q_1)]\}$

$$cf = cf \times m$$

$m = 1 + (\text{MAX}(RH - RH_c, 0)/(RH_{ss} - RH_c))^{1.9}$, where RH is the relative humidity, $RH_c = 0.75$ and $RH_{ss} = 1.01$

Higher-Order Form

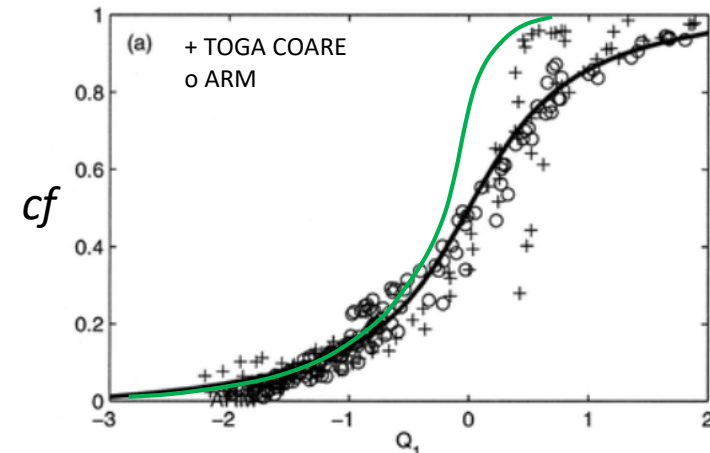
The subgrid variability of the saturation deficit, s , is expressed solely as the square root of the total water variance, q'^2 :

$$\sigma_s = [q'^2]^{1/2},$$

And then the normalized saturation deficit is specified as:

$$Q_1 = (\bar{q}_w - q_{sat}(\bar{T}_l))/\sigma_s.$$

Then, the same cloud fraction function is used as in the first-order form.



Taken from Chaboureaux and Bechtold (2002, JAS)

Introducing a Level 2.6 configuration

- Prognoses **TKE** and q'^2 (instead of just TKE)
- Currently, q'^2 is not advected
 - Makes the increased computational cost very small

- Introduce a new *bl_mynn_closure* namelist variable:

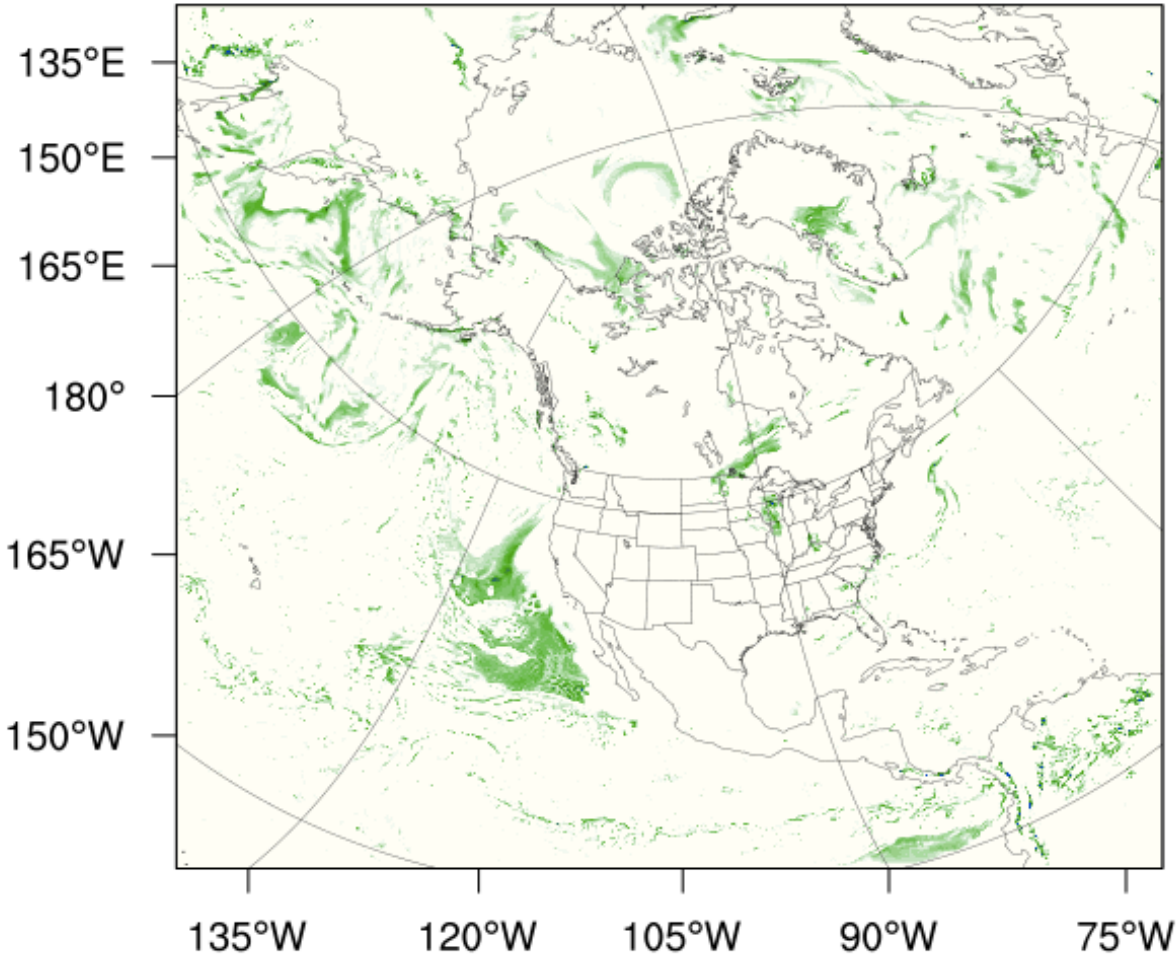
$$\text{Closure} = \begin{cases} \text{level 2.5,} & \text{bl_mynn_closure} \leq 2.5 & \text{(TKE)} \\ \text{level 2.6,} & 2.5 < \text{bl_mynn_closure} < 3.0 & \text{(TKE and } q'^2) \\ \text{level 3.0,} & 3.0 \leq \text{bl_mynn_closure} & \text{(TKE, } q'^2, \theta'q', \text{ and } \theta'^2) \end{cases}$$

- Note: the higher-order (q'^2) cloud PDF can be used with any closure level, but will use the diagnostic form of q'^2 when *bl_mynn_closure* = 2.5

Impact on Diagnosed Cloud Water at 500 m

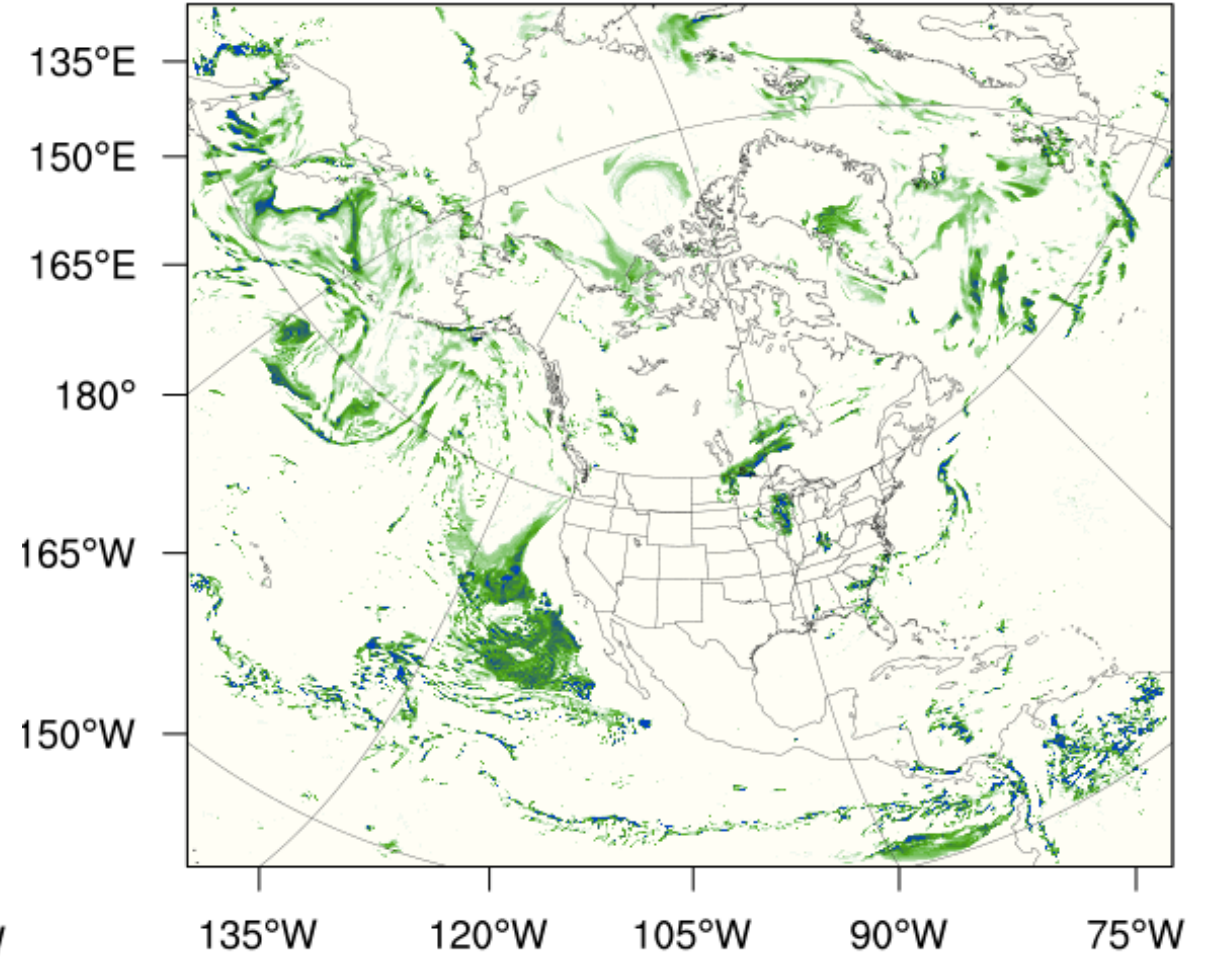
Chab-Bect Qc (kg kg⁻¹)

1st-Order σ_s

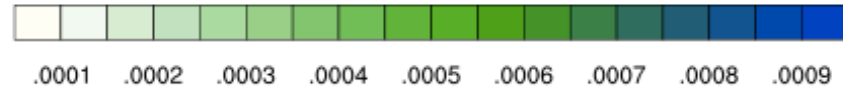


Chab-Bect Qc (kg kg⁻¹)

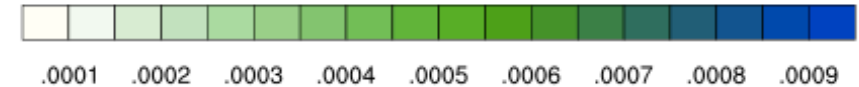
$q'^2 - \sigma_s$



Chab-Bect Qc (kg kg⁻¹)



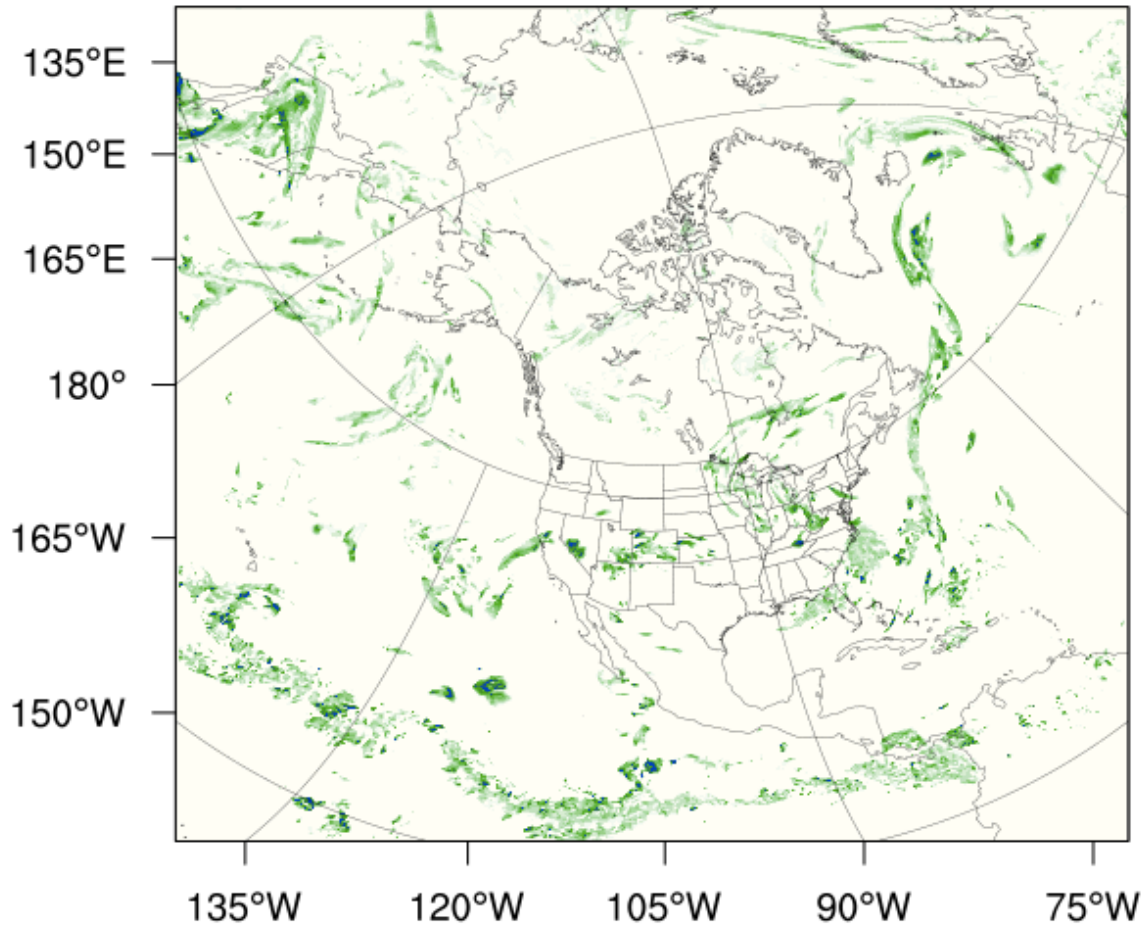
Chab-Bect Qc (kg kg⁻¹)



Impact on Diagnosed Cloud Ice at 300 mb

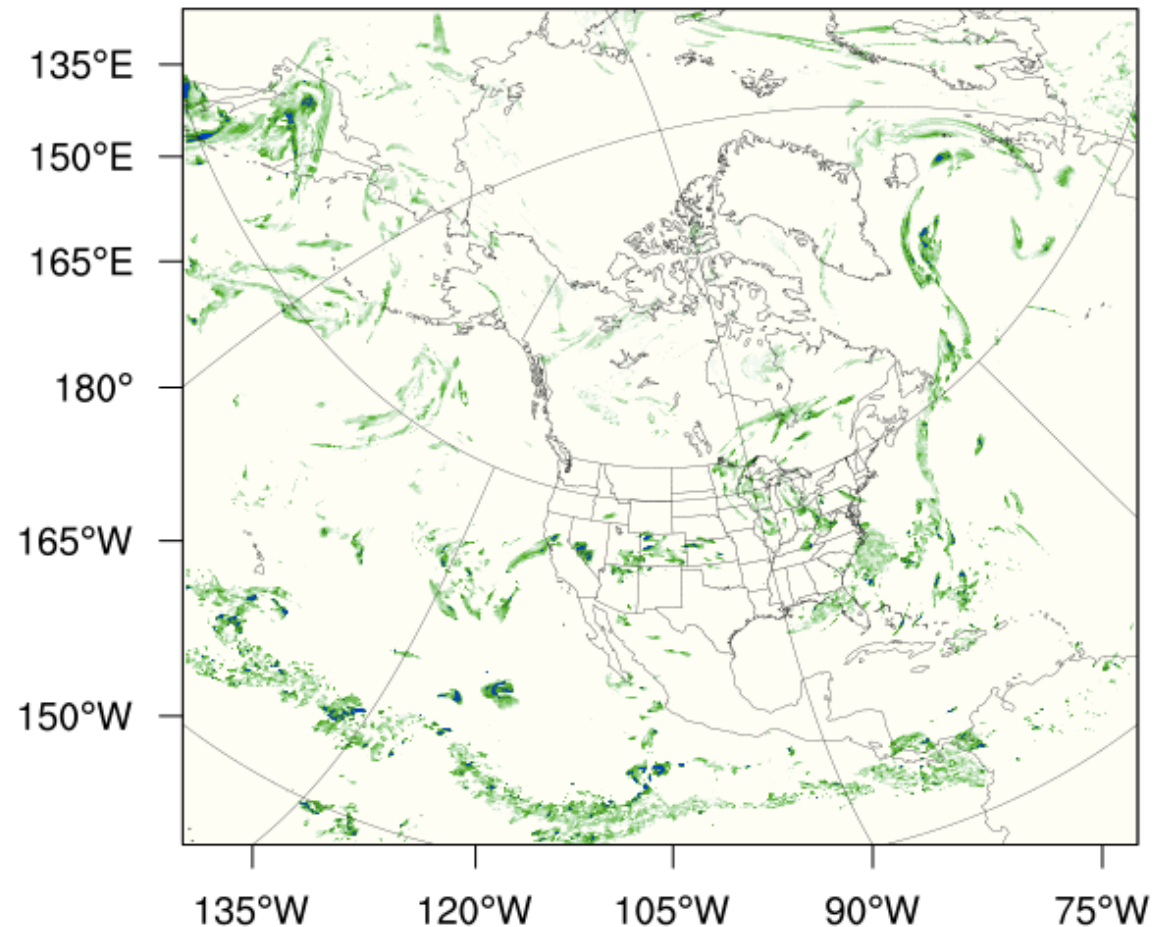
1st-Order σ_s

Chab-Bect Qi (kg kg⁻¹)



$q'^2 - \sigma_s$

Chab-Bect Qi (kg kg⁻¹)



Chab-Bect Qi (kg kg⁻¹)



.00001 .00002 .00003 .00004 .00005 .00006 .00007 .00008 .00009

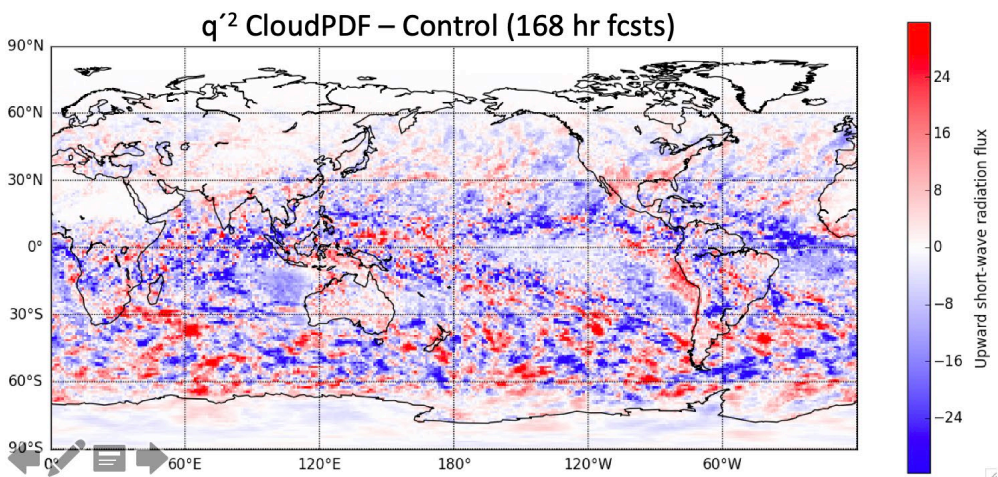
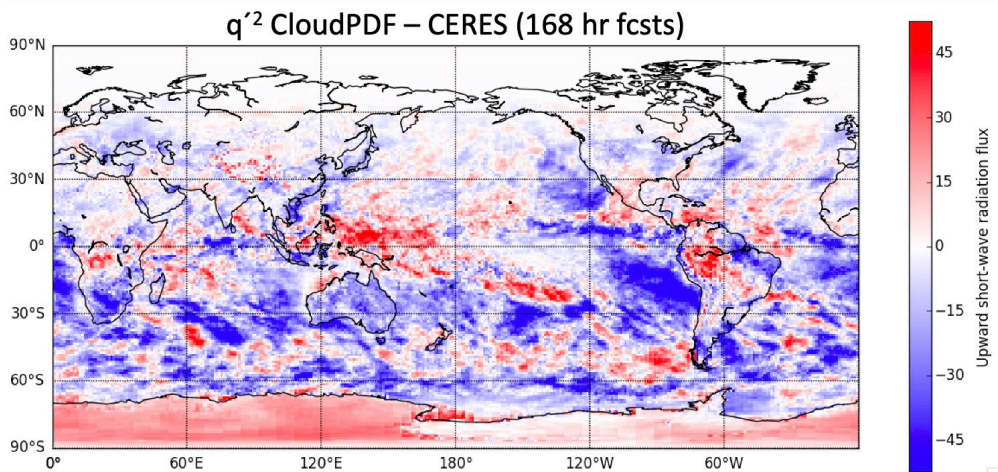
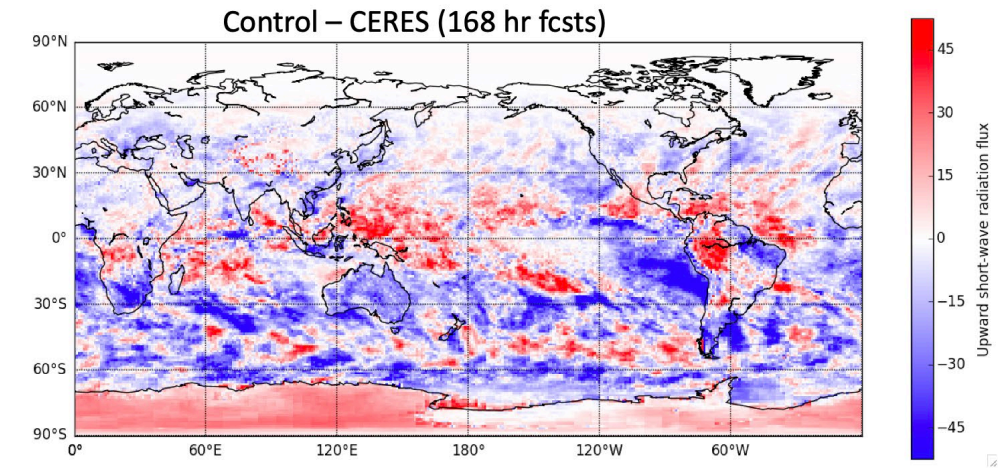
Chab-Bect Qi (kg kg⁻¹)



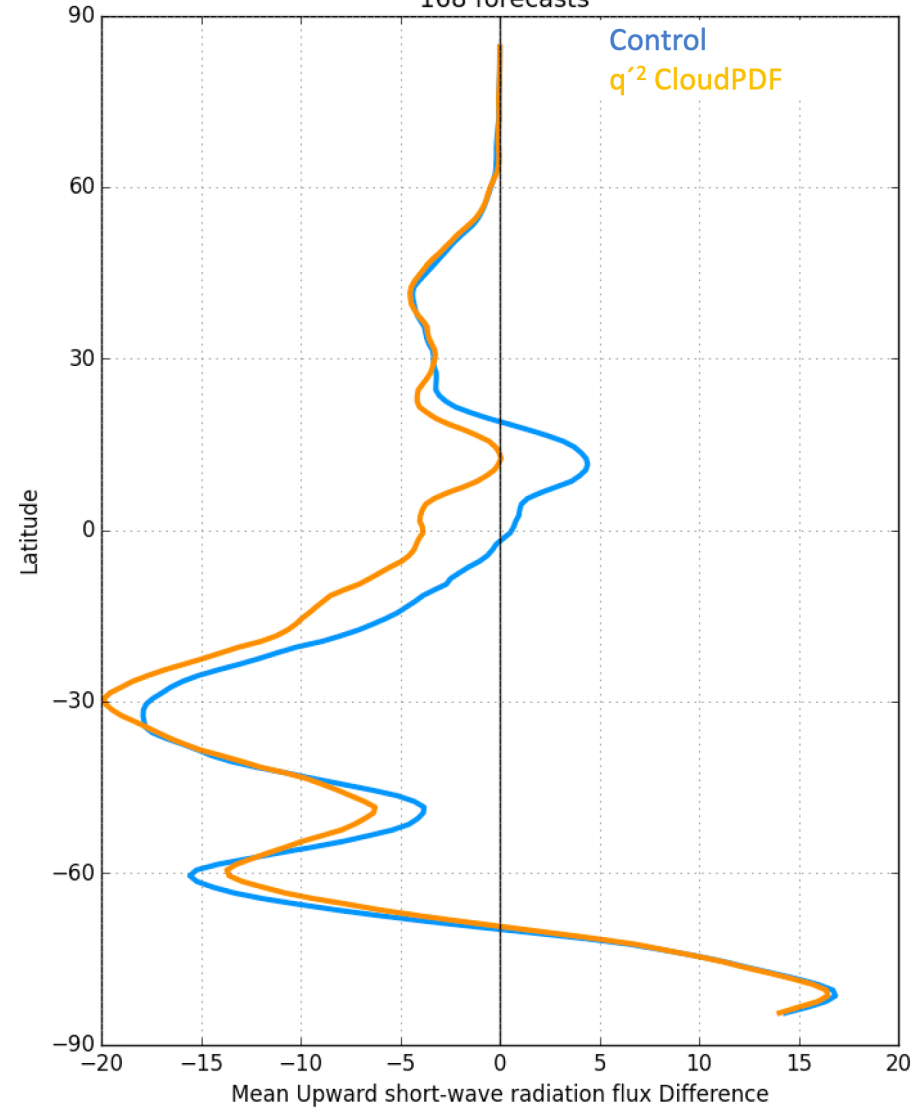
.00001 .00002 .00003 .00004 .00005 .00006 .00007 .00008 .00009

Upward SW Radiation at TOA

20 Oct – 29 Dec, Init every 5 days, Averaging day 6 fcsts

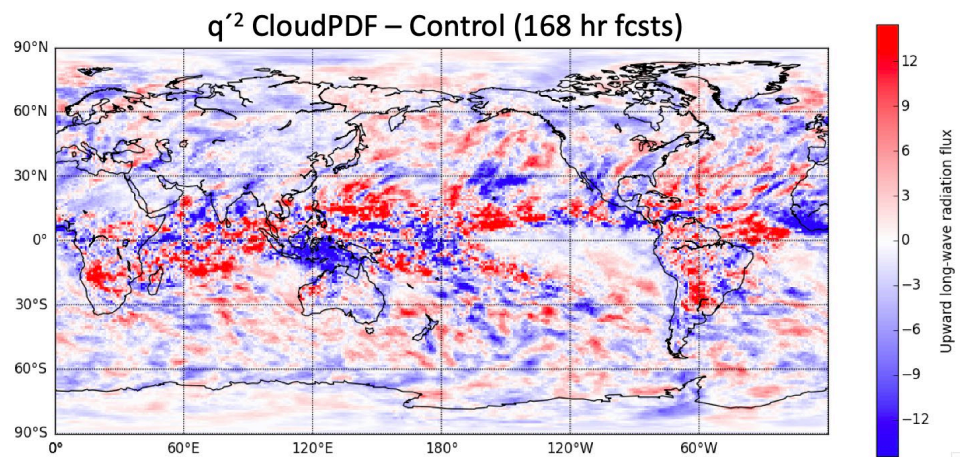
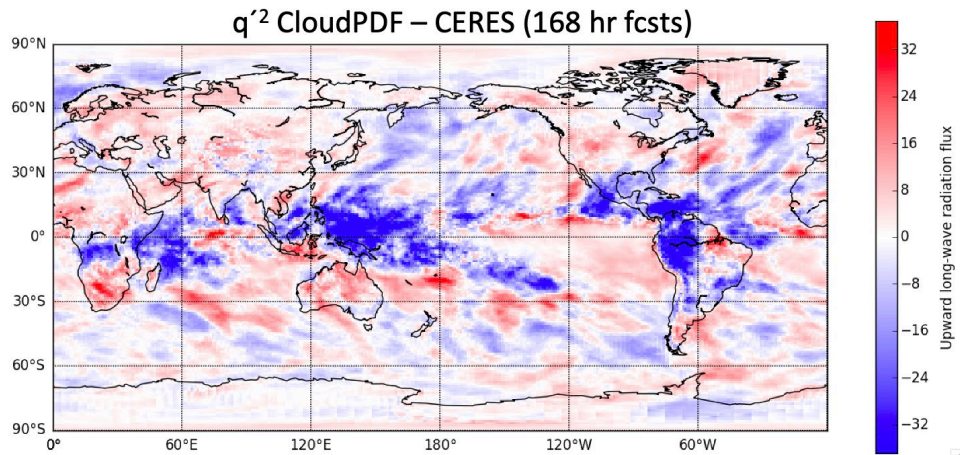
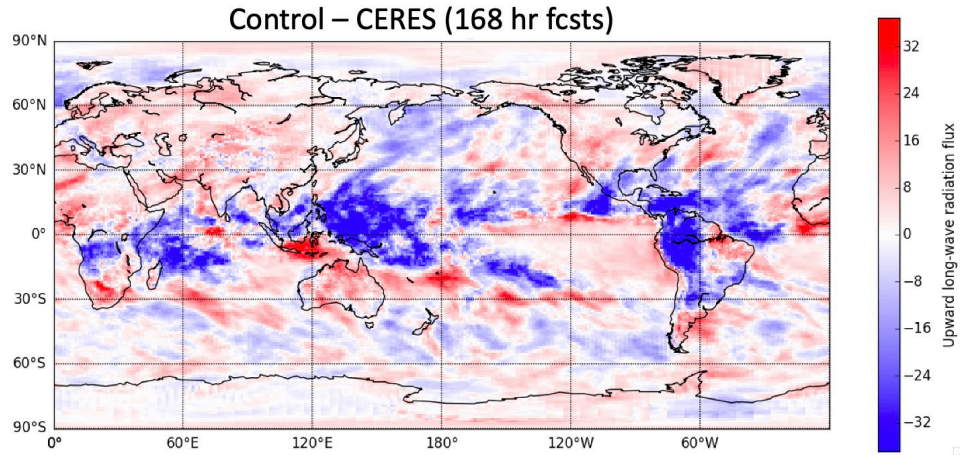


Zonal Average TOA Upward short-wave radiation flux Difference from CERES
168 forecasts

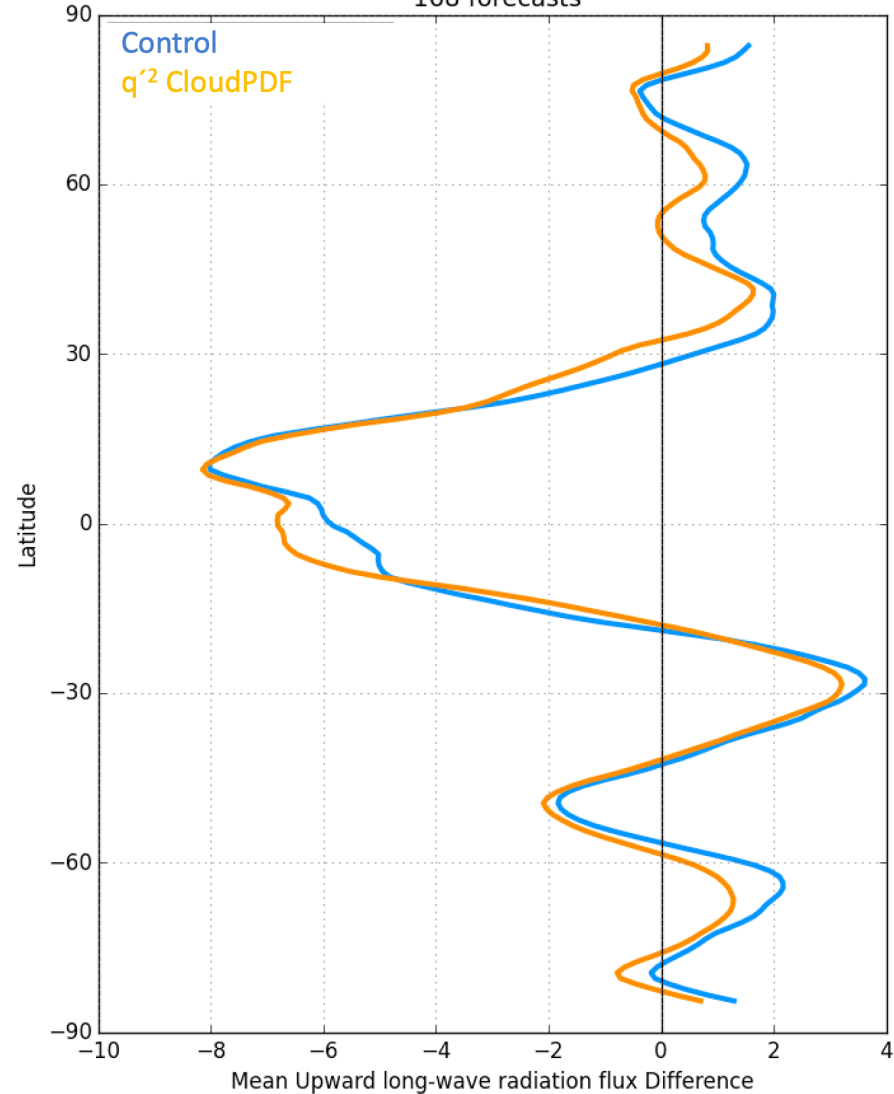


Upward LW Radiation at TOA

20 Oct – 29 Dec, Init every 5 days, Averaging day 6 fcsts



Zonal Average TOA Upward long-wave radiation flux Difference from CERES
168 forecasts



Improvements from Single-Column Modeling

SCM work in WRF and CCM3 has shown:

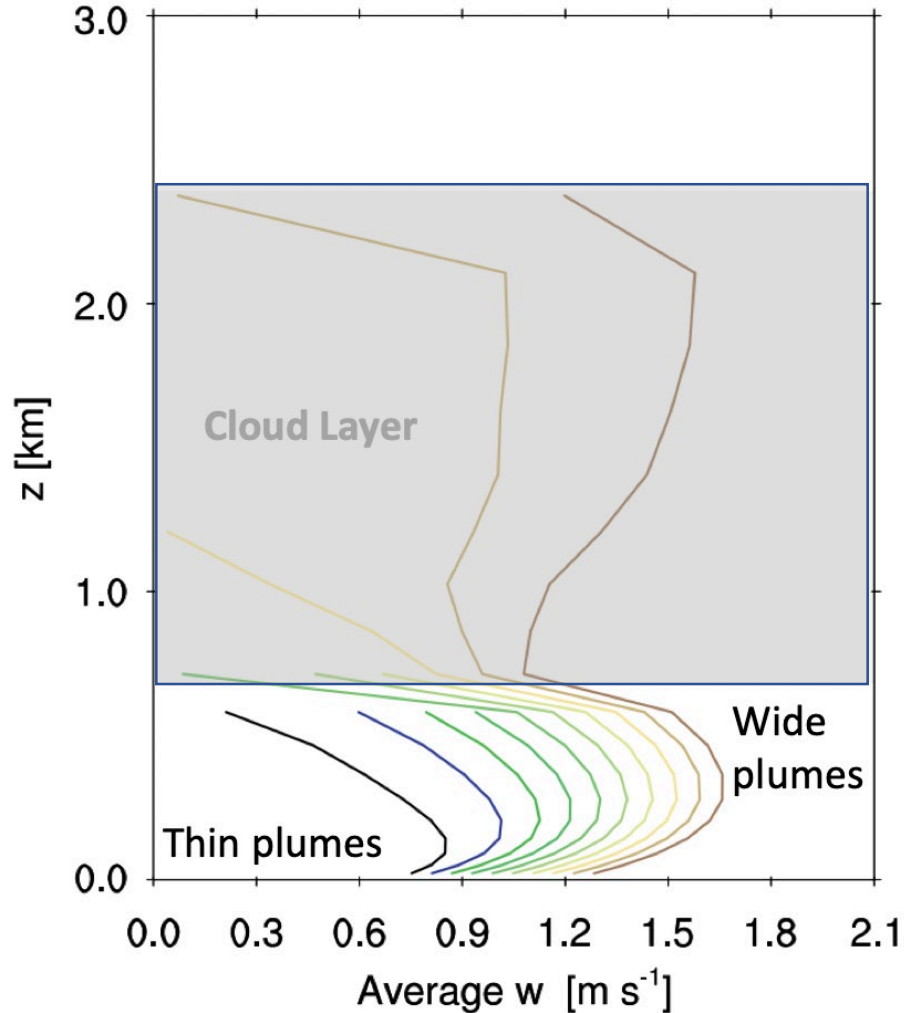
- Good performance for LASSO shallow cumulus cases
- Improved tuning of mass flux component
- Need for more careful consideration of scale-aware features
- Improved understanding of how to specify forcing and interpret SCM results
- Using many cases avoids over-fitting
- Easy testing of different vertical grids
- Built capacity and collaboration among GSL and CSL groups

Publications:

Angevine et al. 2018, Shallow Cumulus in WRF Parameterizations Evaluated against LASSO Large-Eddy Simulations. *Monthly Weather Review*, vol. 146, pp. 4303-4322.

Angevine et al. 2020, Scale Awareness, Resolved Circulations, and Practical Limits in the MYNN-EDMF Boundary Layer and Shallow Cumulus Scheme. *Monthly Weather Review*, vol. 148, pp. 4629-4639.

Accelerating Plume Modification



Adapted from Neggers (2015, JAMES)

The only distinguishing aspect to each plume is the entrainment rate ε_i , which is taken from Tian and Kuang (2016):

$$\varepsilon_i = \frac{C_\varepsilon}{w_i l_i}$$

Where l_i is the plume diameter, and $C_\varepsilon = 0.33$.

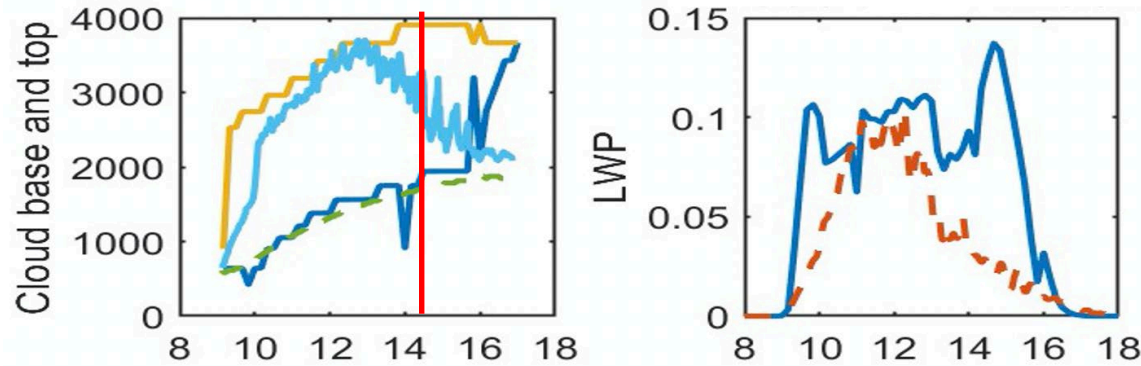
For large plume sizes, this form can produce a positive feedback between large w_i and ε_i , causing shallow cumulus to become too deep.

This modification increases the entrainment in accelerating plumes above the cloud base.

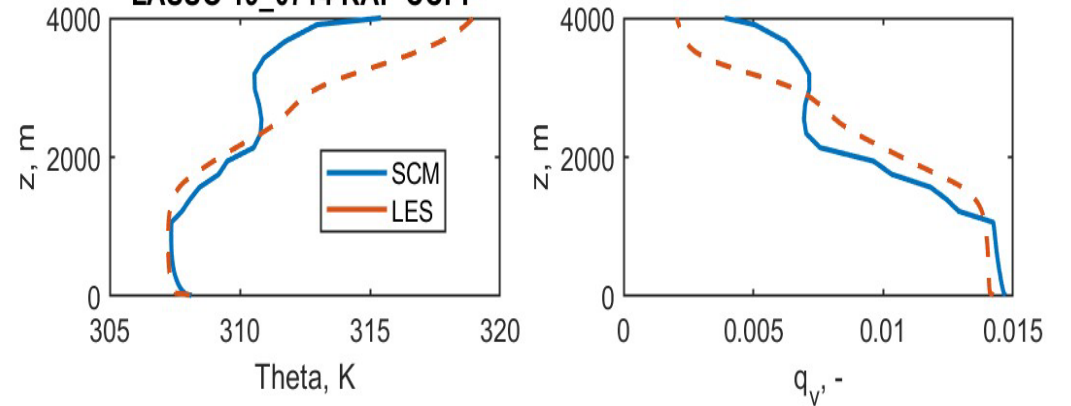
Hereafter, this will be referred to as **the ACP mod.**

Example of improvement with the ACP mod

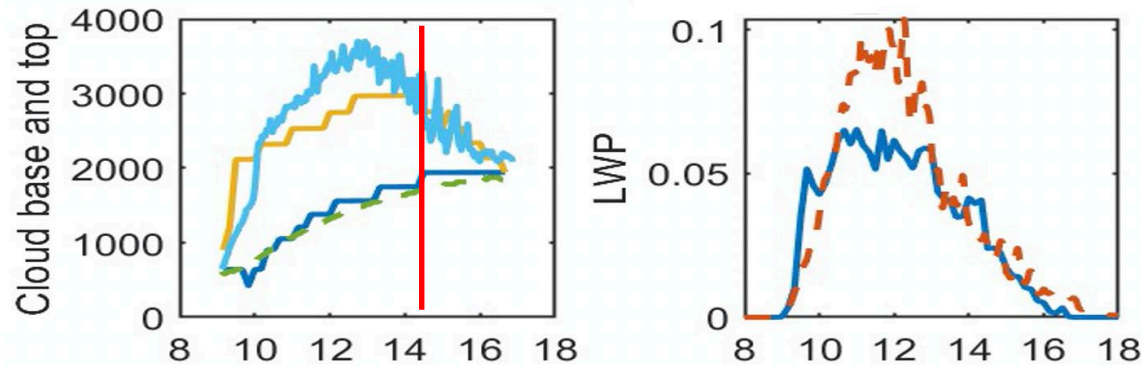
LASSO 14 July 2019



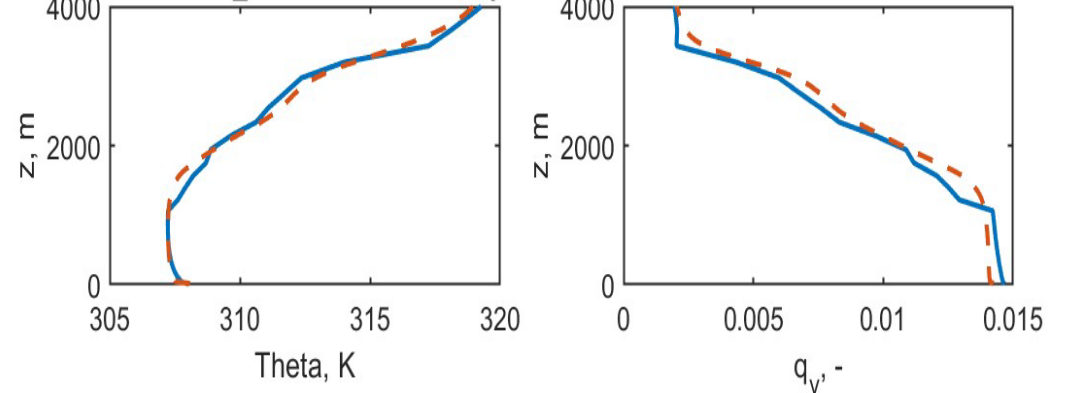
LASSO 19_0714 RAP CCPP



CTL



LASSO 19_0714 RAP CCPP acp



LES Cloud Top
 SCM Cloud Top
 LES Cloud Base
 SCM Cloud base

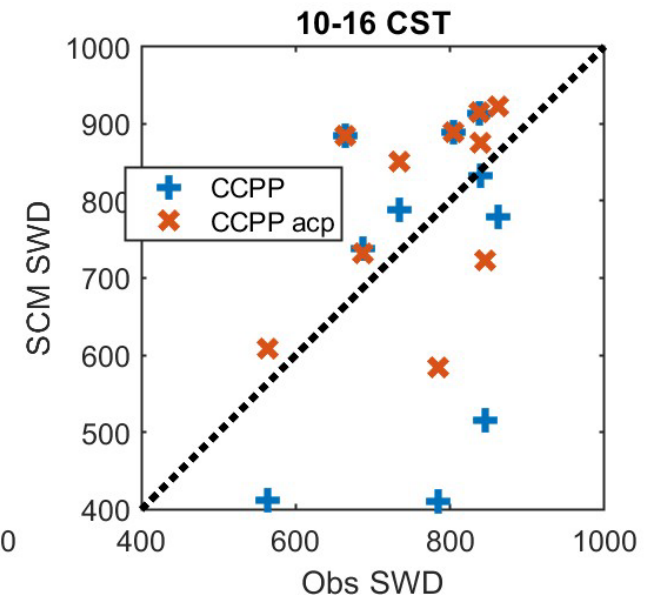
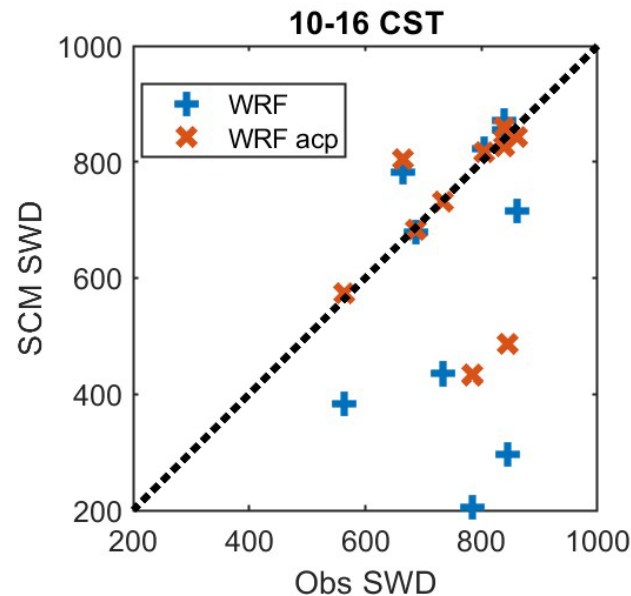
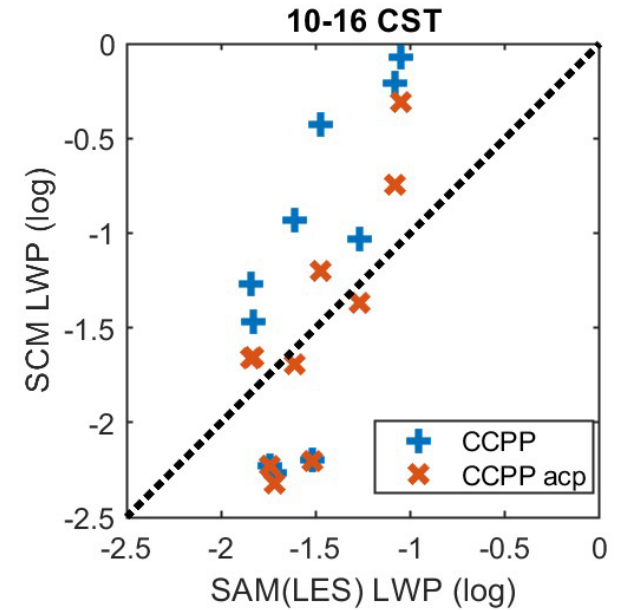
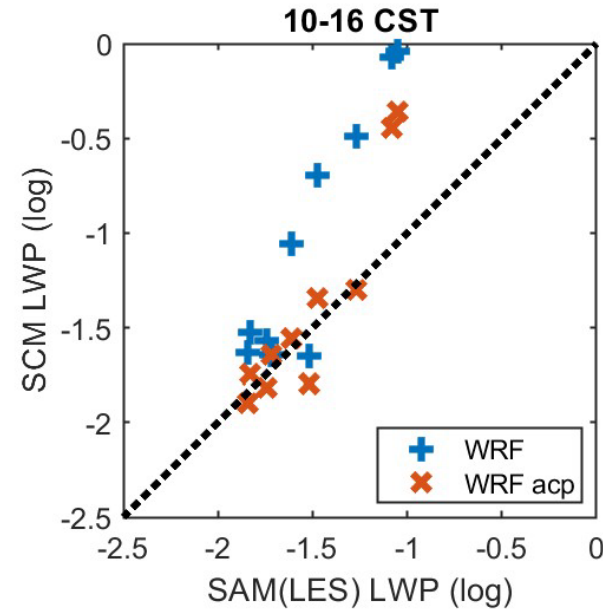
-LES -SCM

- Accelerating plume modification drastically improves LWP and cloud depth evolution (*note different vertical axis scales*)
- Smoother profiles with ACP

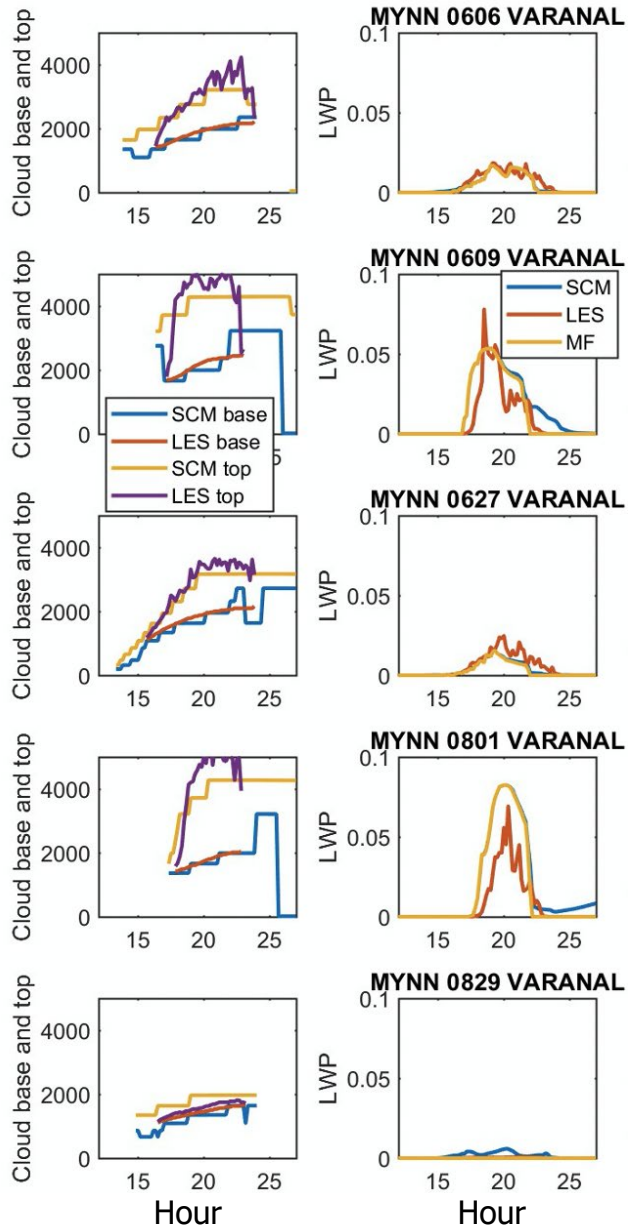
Testing the updated code in both WRF and CCPP

Ten “good” LASSO cases from 2018 and 2019:

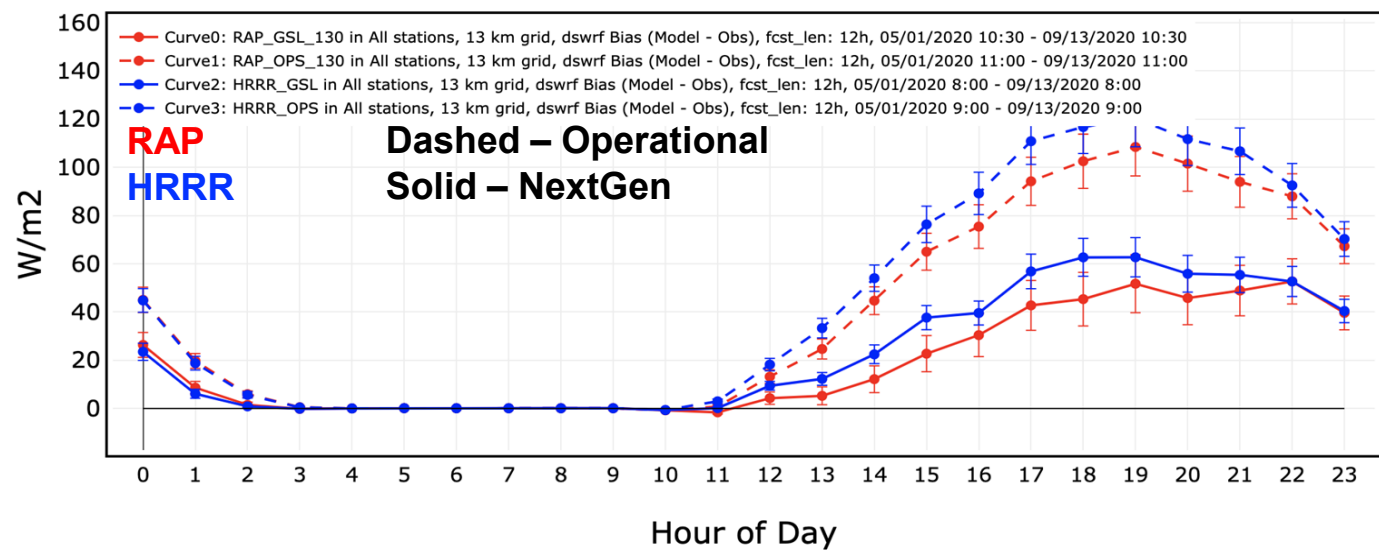
- All SCM cases created from RAP analyses
- WRF and CCPP results are fairly similar
- Caveats: Vertical grids are not identical
- Two cases have far too much cloud (0712 and 1002)
- Accelerating plume mod (“acp”) improves LWP and SWD (see later)



Nice, but we need to do better...



- ✓ Improved shallow-cumulus cloud depth
- ✓ Improved areal coverage
- ✓ Improved LWP
- ✓ Improved specification of effective radii
- ✓ Improved diurnal cycle of shallow cumulus

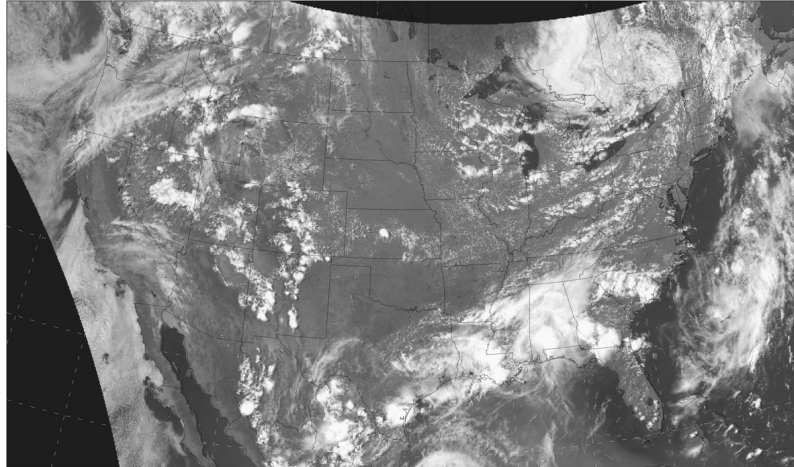


Ongoing/Future Work: Cloud Regime Diagnostic

21 UTC 24 June 2020

GOES-16 combined (ch1, 2, 3) visible albedo

20:52:35 24 Jun 2020



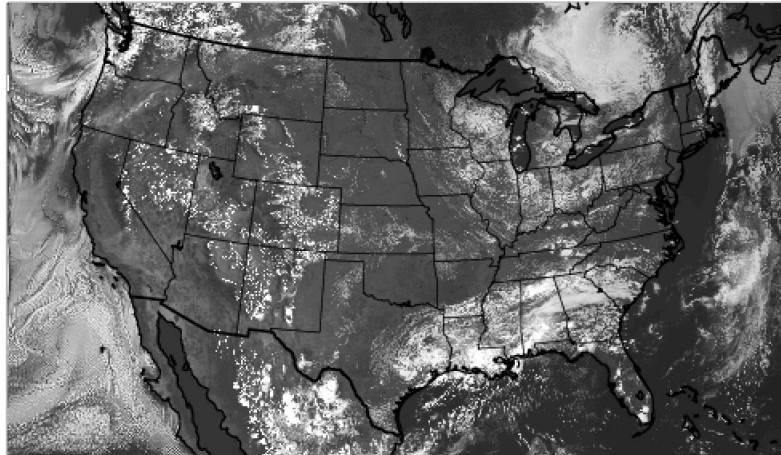
.01.04.07 .1 .13.16.19.22.25.28.31.34.37 .4 .43.46.49.52.55.58.61.64.67 .7 .73.76.79.82.85.88.91.94

HRRR

Upward SW at TOA ($W m^{-2}$)

Init: 2020-06-24_09:00:00

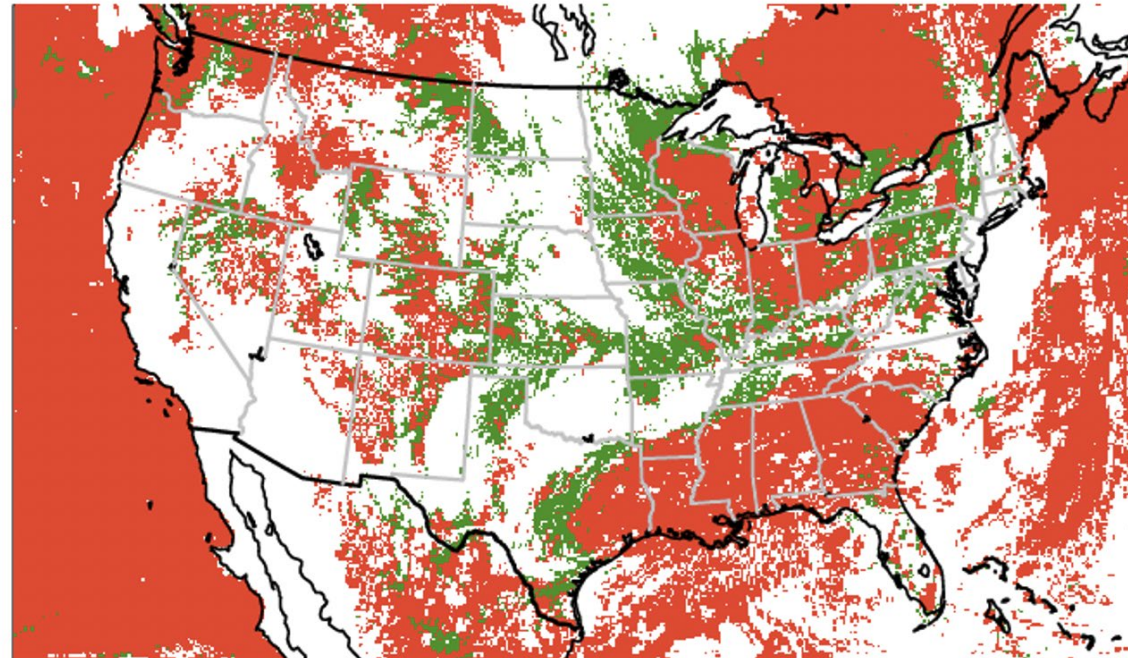
Valid: 2020-06-24_21:00:00



0 50 100 150 200 250 300 350 400 450 500 550 600 650 700 750 800

Cloud Regime

Valid: 2020-06-24_21:00:00



Clear

Pure Shallow
Cumulus

Other

- Better characterize our errors in each regime
- Link the errors to dominant processes in each regime
- Refine the cloud macro- and microphysics in each regime, i.e., cloud fraction, mixing ratios, effective radii, overlap, etc

GOES-16
Satellite

HRRR

Summary

- Development of the MYNN-EDMF has been equally focused on turbulence and cloud-radiative processes, exploiting both mass-flux and HOC.
- Testing in a hierarchy of models: global, regional, and SCM. Using LES as much as observations.
- Numerical pathologies associated with the stability functions have been alleviated
 - Overall improvements were found in bulk global and regional retrospective tests as well as 3D and SCM case studies
- Excessive cloudiness in the shallow-cumulus regime was caused by a positive feedback between the plume entrainment and vertical velocity
 - Modified entrainment in accelerating moist plumes addresses this problem
 - Improvements in LWP and SW-down were demonstrated
- Future work is planned to better sort the radiation errors by cloud regime and investigate the cloud-overlap in shallow-cumulus regimes

Extra slides

TKE Budget Fixes

Important fixes from Franciano Puhales:

- Vertical Transport term
- Vertical indexing
- Now accurate to within the level of noise.

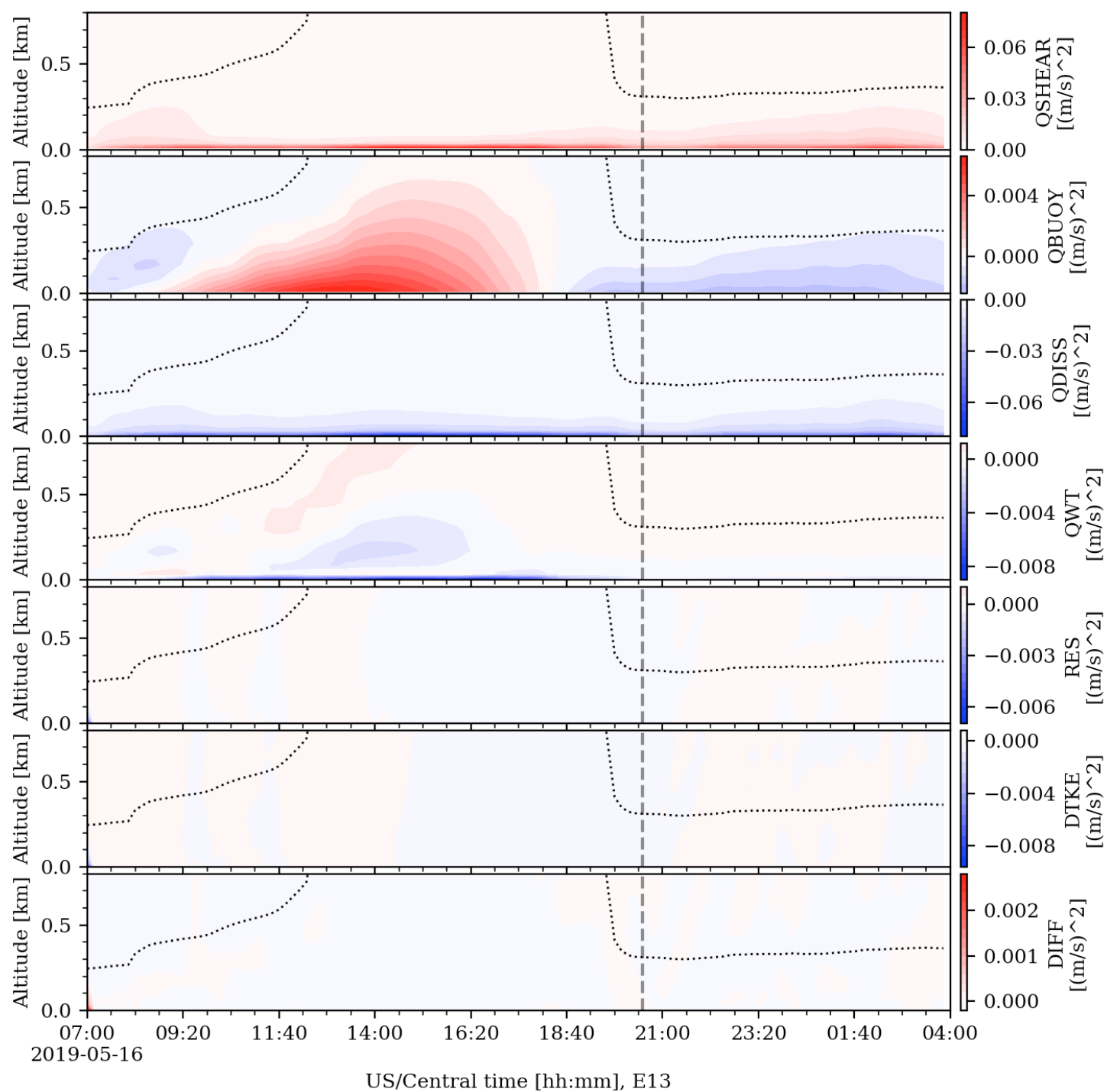
$$\frac{\partial q^2}{\partial t} = -\frac{\partial}{\partial z} \langle w(u^2 + v^2 + w^2 + 2p/\rho_0) \rangle - 2 \left(\langle uw \rangle \frac{\partial U}{\partial z} + \langle vw \rangle \frac{\partial V}{\partial z} \right) + 2 \frac{g}{\Theta_0} \langle w\theta_V \rangle - 2\varepsilon.$$

\downarrow \downarrow \downarrow \downarrow
 RES = QWT + QSHEAR + QBUOY + QDISS

DTKE = TKE_t - TKE_{t-1}

and

DIFF = RES - DTKE (well in the noise)



Example Comparison of SW-up at Top of Atmosphere

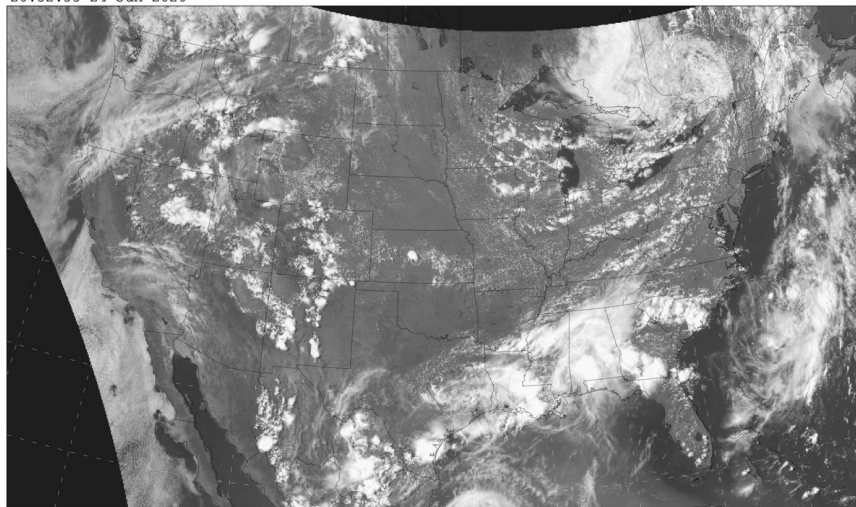
21 UTC 24 June 2020

Forecast hour 12, Initialized 09 UTC 24 June 2020

**GOES-16
Satellite**

GOES-16 combined (ch1, 2, 3) visible albedo

20:52:35 24 Jun 2020



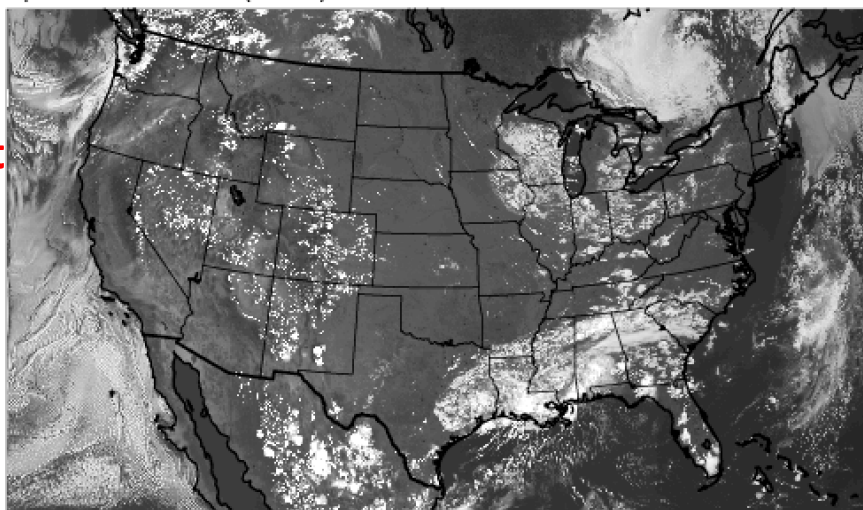
.01 .04 .07 .1 .13 .16 .19 .22 .25 .28 .31 .34 .37 .4 .43 .46 .49 .52 .55 .58 .61 .64 .67 .7 .73 .76 .79 .82 .85 .88 .91 .94

HRRR

Upward SW at TOA ($W m^{-2}$)

Init: 2020-06-24_09:00:00

Valid: 2020-06-24_21:00:00

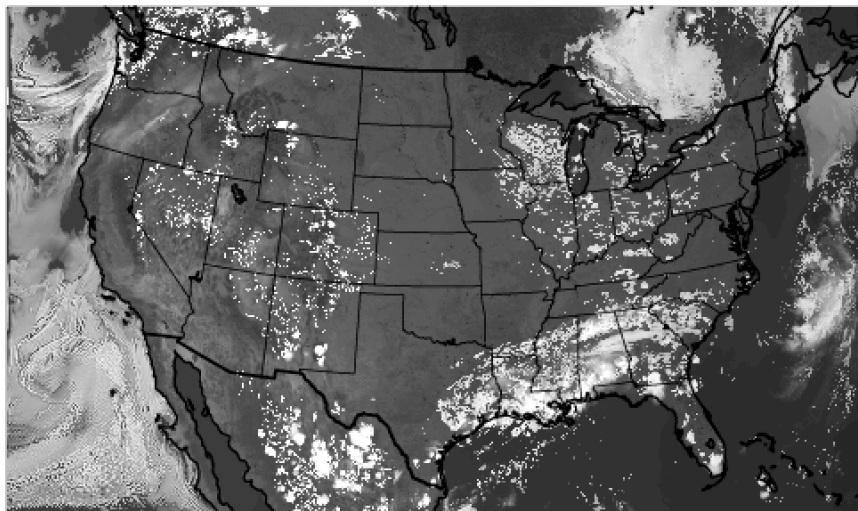


HRRR

Upward SW at TOA ($W m^{-2}$)

Init: 2020-06-24_09:00:00

Valid: 2020-06-24_21:00:00



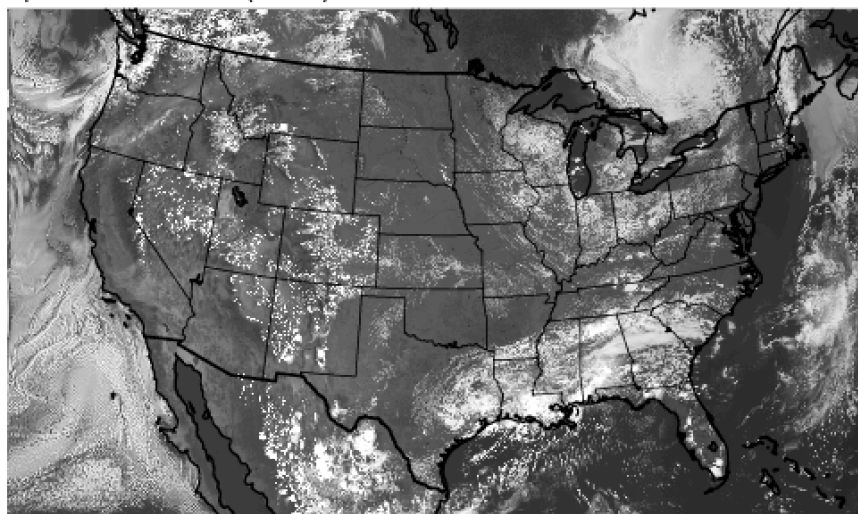
**No SGS Clouds – all
clouds are from the
Thompson
microphysics scheme**

HRRR

Upward SW at TOA ($W m^{-2}$)

Init: 2020-06-24_09:00:00

Valid: 2020-06-24_21:00:00



**Both Stratus +
Mass-Flux components**



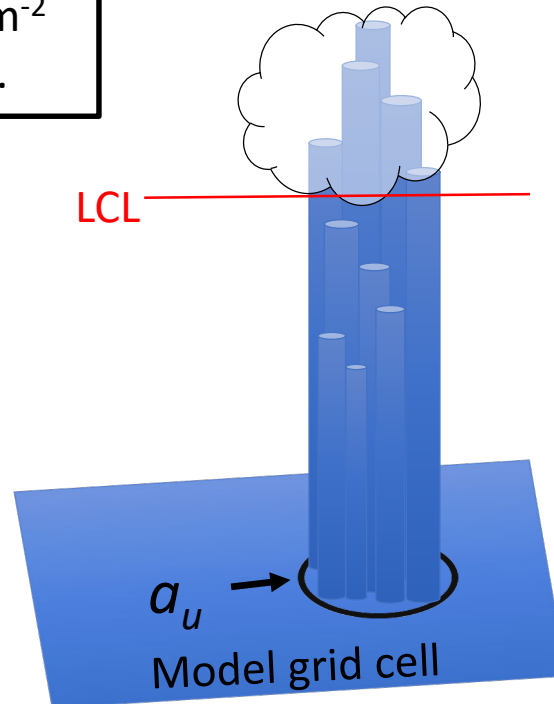
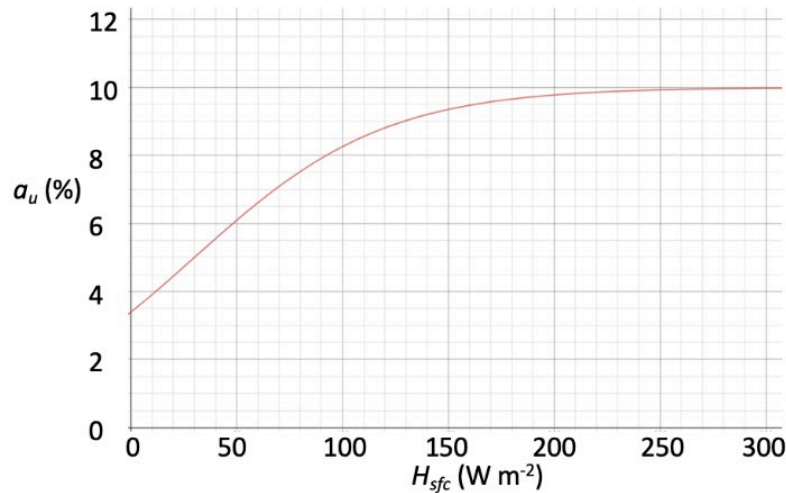
**Stratus
component
only**

Mapping the contribution of each plume to the total fractional area

The fraction grid area assumed to contain coherent updrafts, a_u (%), is set to be proportional to the surface buoyancy flux (H_{sfc} , $W m^{-2}$):

$$a_u = 10.0\{0.5 \tanh[(H_{sfc} - 30)/90] + .5\},$$

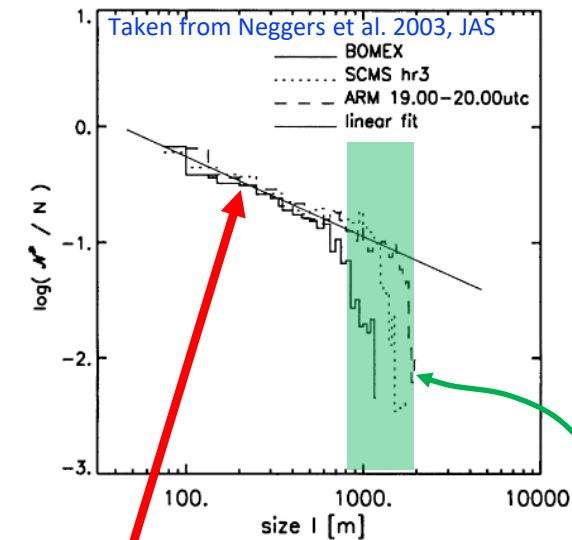
a_u varies between $\sim 10\%$ for $H_{sfc} > 200 W m^{-2}$ and as small as 3-4% for H_{sfc} near $0 W m^{-2}$.



The number density, \mathcal{N} , of plume sizes is represented by a power law:

$$\mathcal{N}(\ell) = C\ell^d$$

where C is a constant of proportionality, ℓ is the diameter of the plume, and d is the slope of the power-law relationship. \mathcal{N} effectively weights the contribution each plume size in a_u :



Note:
 For $d < -2$, smaller plumes dominate a_u
 For $d > -2$, larger plumes dominate a_u

The slope (d) is -1.9 ± 0.3 for the scales below the *scale break*.

Chaboureau and Bechtold Subgrid Cloud Fraction: Stratus & Convective components

Stratus Component

The subgrid variability of the saturation deficit, s , is expressed in terms of the total water and liquid water temperature:

$$\sigma_{s-strat} = c_\sigma l \left(\bar{a}^2 \left(\frac{\partial \bar{r}_w}{\partial z} \right) - 2\bar{a}\bar{b}C_{pm}^{-1} \frac{\partial \bar{h}_l}{\partial z} \frac{\partial \bar{r}_w}{\partial z} + \bar{b}^2 C_{pm}^{-2} \left(\frac{\partial \bar{h}_l}{\partial z} \right)^2 \right)^{1/2}$$

Where c_σ is a tuning constant, l is the mixing length, and a and b are thermodynamic functions arising from the linearization of the function for the water vapor saturation mixing ratio.

Convective Component

The subgrid variability of the saturation deficit is proportional to the mass-flux, M :

$$\sigma_{s-conv} \approx M \frac{(s^c - s^e)}{w_* \rho_*} \approx \alpha M f(z/z^*)$$

Where α is a constant of proportionality ($\approx 6E-3$) and f is a vertical scaling function, set to $f = \bar{a}^{-1}$.

Combined saturation deficit variance \longrightarrow $\sigma_{s-conv} = \sqrt{\sigma_{s-strat}^2 + \sigma_{s-conv}^2}$

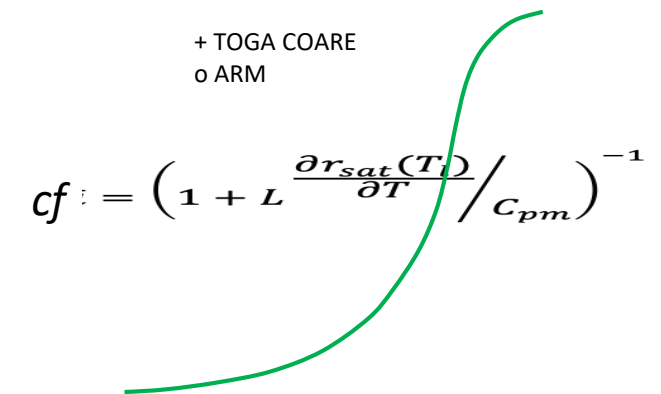
$$\bar{a} = \left(1 + L \frac{\partial r_{sat}(T_l)}{\partial T} / C_{pm} \right)^{-1} \quad \bar{b} = \bar{a} \frac{\partial r_{sat}(T_l)}{\partial T}$$

Normalized saturation deficit \longrightarrow $Q_1 = \bar{a}(\bar{r}_w - r_{sat}(\bar{T}_l)) / \sigma_{s-x}$

Subgrid cloud fraction \longrightarrow $cf = \text{MAX}\{0, \text{MIN}[1, 0.5 + 0.36 \text{ATAN}(1.55 Q_1)]\}$

$$cf_+ = cf \times m$$

$$m = 1 + (\text{MAX}(RH - RH_c, 0)) / (RH_{ss} - RH_c)^{1.9}, \text{ where } RH \text{ is the relative humidity, } RH_c = 0.75 \text{ and } RH_{ss} = 1.01$$



Taken from Chaboureau and Bechtold (2002, JAS)